

Supporting Information

Light-Harvesting Systems Based on Organic Nanocrystals To Mimic Chlorosomes

*Peng-Zhong Chen, Yu-Xiang Weng, Li-Ya Niu, Yu-Zhe Chen, Li-Zhu Wu, Chen-Ho Tung, and Qing-Zheng Yang**

anie_201510503_sm_miscellaneous_information.pdf

Supporting Information

Contents

1. Materials and Methods.....	S2
2. Synthesis of chromophores and preparation of nanocrystals	
(1) Synthesis of BF ₂ bcz, BF ₂ cna and BF ₂ dan.....	S3 – S7
(2) Preparation of nanocrystals and their reproducibility.....	S7 – S8
3. Characterization of nanocrystals and spectroscopies of chromophores and nanocrystals	
(1) Figure S2 – S11.....	S9 – S12
(2) Table S1.....	S13
(3) Figure S12 – S17.....	S14 – S17
4. The single crystal data of BF ₂ bcz and NMR and HR-ESI spectra of chromophores	
(1) Table S2.....	S18
(2) The ¹ H NMR spectra of compounds 2, 3, 5, 6, 8, 9 and 11-13.....	S19 – S23
(3) The ¹ H NMR, ¹³ C NMR and HR-ESI spectra of BF ₂ bcz, BF ₂ cna and BF ₂ dan....	S23 – S27
5. The lifetime decay profiles of nanocrystals with different ratios of acceptors.....	S28 – S31
6. References.....	S32

1. Materials and Methods

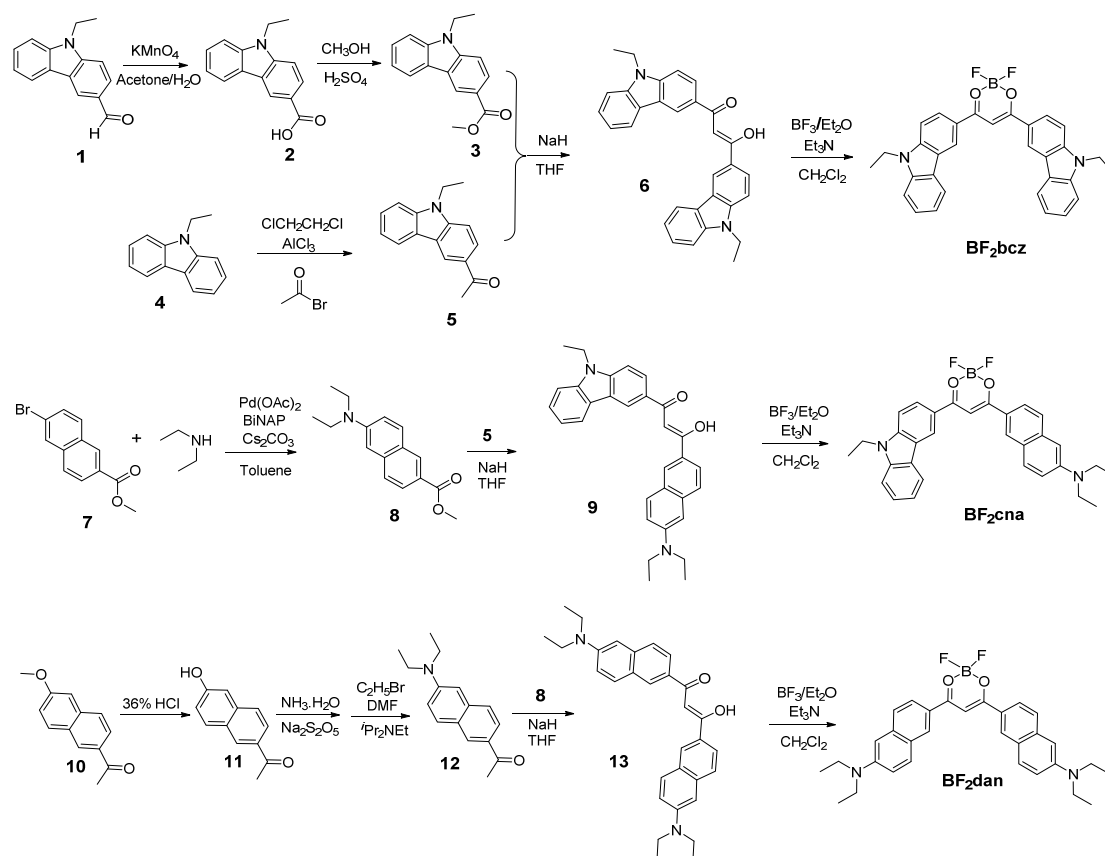
Unless otherwise noted, all chemicals were commercially available and were used without further purification. High-purity water (resistivity = 18.2 M Ω .cm) was produced with Milli-Q apparatus (Millipore, America) and filtered using an inorganic membrane with a pore size of 0.22 μ m (Whatman International, Ltd) just before use.

^1H and ^{13}C NMR spectra were performed on a Bruker Avance 400 spectrometer. Chemical shifts were reported in ppm and coupling constants (J) were reported in Hz. High-resolution mass spectrometry experiments were performed with Thermo Fisher Q-Exactive or Bruker Apex IV FTMS. The absorbance and fluorescence spectra were recorded on Hitachi U-3900 UV-VIS spectrophotometer and F-4600 fluorescence spectrophotometer respectively at room temperature. Fluorescence decay surfaces were determined by single photon counting technique using a FLS920 Edinburgh spectrometer. Fluorescence microscopy images were performed with Olympus IX 71.

For scanning electron microscopic (SEM) studies, a few drops of the sample were placed onto silicon substrates and the solvent was evaporated at room temperature. The samples were then examined with a field emission SEM (Hitachi S-4300) operated at an accelerating voltage of 10 kV. To minimize sample charging, an ultra-thin layer of Au was deposited onto the samples before SEM examination. Samples for transmission electron microscopy (TEM) were prepared by placing a drop of suspension on a copper grid coated with carbon film, and then dried in air for 24 hours. The TEM study was performed in a JEOL-2100 microscope operated at an accelerating voltage of 200 kV. The powder X-ray diffraction (XRD) patterns of samples were collected on a Bruker D8 Focus X-ray diffractometer with Cu K α radiation (λ = 1.5405 Å) at a scanning rate of 0.05° s $^{-1}$.

2. Synthesis of chromophores and preparation of nanocrystals

(1) Synthesis of BF₂bcz, BF₂cna and BF₂dan.



Synthesis of **2**^[1]: To a solution of **1** (223 mg, 1.0 mmol) in 20 mL acetone/H₂O (1/1, v/v) was added potassium permanganate (315 mg, 2.0 mmol) in three portions. The resulting mixture was stirred at room temperature for 5 hours and followed by filtration through Buchner funnel. The filtrate was concentrated under vacuum to remove acetone and the resulting aqueous solution was acidified with diluted hydrochloric acid to pH = 2. After standing for 1 hour, the precipitated product was collected and dried overnight in vacuum oven to afford the product **2** as white solid (236 mg, 99%). ¹H NMR (400 MHz, DMSO-d₆): δ (ppm) = 12.65 (s, 1H), 8.80 (d, 1H, *J* = 1.6 Hz), 8.28 (d, 2H, *J* = 8.0 Hz), 8.07 (dd, 1H, *J* = 1.6 Hz, 8.0 Hz), 7.70 (d, 1H, *J* = 8.0 Hz), 7.66 (d, 1H, *J* = 8.0 Hz), 7.50 (t, 1H, *J* = 8.0 Hz), 7.27 (t, 1H, *J* = 8.0 Hz), 4.50 (q, 2H, *J* = 7.2 Hz), 1.33 (t, 3H, *J* = 7.2 Hz). HR-ESI-MS: *m/z* [M + H] calculated for C₁₅H₁₄NO₂, 240.1025; found, 240.1014.

Synthesis of **3**: To a solution of compound **2** (120 mg, 0.5 mmol) in 10 mL methanol was added 1 mL concentrated sulfuric acid. The resulting solution was stirred at 60 °C. The reaction was monitored by TLC analysis until completed. After cooling to room temperature, the reaction solution was concentrated under reduced pressure, and the residue was diluted with dichloromethane, followed by washing with NaHCO₃ solution and brine twice respectively. The organic layers was dried over anhydrous Na₂SO₄ and concentrated under reduced pressure. The crude product was purified by column chromatography (silica gel,

1:1 v/v, petroleum ether/dichloromethane) to afford **3** as white solid (120 mg, 94%). ¹H NMR (400 MHz, CDCl₃): δ (ppm) = 8.70 (s, 1H), 8.02 (t, 2H, *J* = 9.6 Hz), 7.36 (t, 1H, *J* = 7.2 Hz), 7.26 (d, 1H, *J* = 8.4 Hz), 7.22 (d, 1H, *J* = 8.4 Hz), 7.16 (t, 1H, *J* = 7.2 Hz), 4.18 (q, 2H, *J* = 6.8 Hz), 3.85 (s, 3H), 1.28 (t, 3H, *J* = 6.8 Hz). HR-ESI-MS: *m/z* [M + H] calculated for C₁₆H₁₆NO₂, 254.1181; found, 254.1169.

Synthesis of **5**^[2]: To a solution of **4** (200 mg, 1.0 mmol) in 10 mL 1,2-dichloroethane was added AlCl₃ (650 mg, 5 mmol) and acetyl bromide (80 μL, 1.0 mmol). The reaction mixture was stirred at room temperature for 5 hours, and then poured into 20 mL diluted HCl ice water. The organic phase was collected, dried over anhydrous Na₂SO₄ and concentrated in vacuum. The crude product was purified by column chromatography (silica gel, 2:1 v/v, petroleum ether/dichloromethane) to afford **5** as yellow grey solid (177 mg, 74%). ¹H NMR (400 MHz, CDCl₃): δ (ppm) = 8.72 (s, 1H), 8.05 (q, 2H, *J* = 7.2 Hz), 7.50 (t, 1H, *J* = 7.2 Hz), 7.42 (d, 1H, *J* = 8.4 Hz), 7.35 (d, 1H, *J* = 8.4 Hz), 7.30 (t, 1H, *J* = 7.2 Hz), 4.30 (q, 3H, *J* = 7.2 Hz), 2.71 (s, 3H), 1.42 (t, 3H, *J* = 7.2 Hz). HR-ESI-MS: *m/z* [M + H] calculated for C₁₆H₁₆NO, 238.1232; found, 238.1221.

Synthesis of **6**: To a three-necked flask was added compound **5** (118 mg, 0.5 mmol) in 5 mL anhydrous THF. The solution was purged with N₂ for 10 min, and then added NaH (57-63% oil dispersion, 200 mg, 5.0 mmol). After stirring for 30 min under N₂ at 65 °C, to the reaction mixture was added compound **3** (125 mg, 0.5 mmol) in 5 mL THF via syringe pump over the course of 30 minutes. The reaction mixture was stirred for 24 hours at 65 °C under N₂ protection. After cooling to room temperature, the reaction was quenched by addition of water carefully in an ice bath. The pH was adjusted to 3 with HCl (aq). THF was removed under reduced pressure, and the aqueous suspension was extracted with dichloromethane. The combined organic phase was dried over anhydrous Na₂SO₄, and concentrated under reduced pressure. The crude product was purified by column chromatography (silica gel, 10:1 v/v, petroleum ether/ethyl acetate) to afford product **6** as yellow solid (90 mg, 39.2%). ¹H NMR (400 MHz, CDCl₃): δ (ppm) = 17.64 (s, 1H), 8.51 (s, 2H), 8.23 (d, 2H, *J* = 7.6 Hz), 8.20 (dd, 2H, *J* = 8.4 Hz, 1.6 Hz), 7.53 (t, 2H, *J* = 8.0 Hz), 7.47 (t, 2H, *J* = 8.0 Hz), 7.31 (t, 3H, *J* = 8.0 Hz), 7.14 (s, 1H), 4.43 (q, 4H, *J* = 7.2 Hz), 1.50 (t, 6H, *J* = 7.2 Hz). HR-ESI-MS: *m/z* [M + H] calculated for C₃₁H₂₇N₂O₂, 459.2073; found, 459.2046.

Synthesis of **BF₂bcz**: To a solution of compound **6** (46 mg, 0.1 mmol) in 5 mL CH₂Cl₂ was added Et₃N (42 μL, 0.3 mmol). After stirring for 10 min at room temperature, BF₃/Et₂O (40 μL, 0.3 mmol) was added. The solution was stirred for another 2 hours in the dark. Water was added to the solution, and the organic layers was collected, washed with water, dried over anhydrous Na₂SO₄, and concentrated under reduced pressure. The crude product was purified by column chromatography (silica gel, 1:1 v/v, petroleum ether/dichloromethane) to afford product **BF₂bcz** as orange solid (40 mg, 80%). ¹H NMR (400 MHz, DMSO-*d*₆): δ (ppm) = 9.31 (s, 1H), 8.48 (d, 2H, *J* = 9.2 Hz), 8.42 (d, 2H, *J* = 8.0 Hz), 8.06 (s, 1H), 7.86 (d, 2H, *J* = 9.2 Hz), 7.74 (d, 2H, *J* = 8.0 Hz), 7.58 (t, 2H, *J* = 7.6 Hz), 7.38 (t, 2H, *J* = 7.6 Hz), 4.58 (q, 4H, *J* = 7.2 Hz), 1.38 (t, 6H, *J* = 7.2 Hz). ¹³C NMR (100

MHz, DMSO- d_6): δ (ppm) = 179.78, 143.68, 140.48, 127.08, 126.82, 123.02, 122.88, 122.39, 122.04, 121.12, 120.58, 110.15, 109.86, 92.34, 37.54, 13.78. HR-ESI-MS: m/z [$M + H$] calculated for $C_{31}H_{26}BF_2N_2O_2$, 507.2055; found, 507.2046.

Synthesis of 8: A thick-wall flask containing compound **7** (530 mg, 2.0 mmol), diethylamine (4.0 mL, 40 mmol) and Cs_2CO_3 (1000 mg, 3.1 mmol) in 10 mL anhydrous toluene was purged with Ar for 20 minutes at room temperature. To the above mixture was added $Pd(OAc)_2$ (25 mg, 0.12 mmol) and (\pm)-2,2'-Bis(diphenylphosphino)-1,1'-binaphthalene (BiNAP, 60 mg, 0.1 mmol). The flask was purged with Ar for another 5 min, and then sealed. The reaction mixture was stirred at 110 °C for 30 hours. After cooling to temperature, 50 mL saturated sodium bicarbonate aqueous solution was added to the reaction mixture. The resulting mixture was extracted with ethyl acetate and the organic phase was separated, dried over anhydrous Na_2SO_4 , and concentrated under reduced pressure. The crude product was purified by column chromatography (silica gel, 1:50 to 1:10 v/v, ethyl acetate/petroleum ether) to afford the product **8** as white solid (250 mg, 48%). 1H NMR (400 MHz, $CDCl_3$): δ (ppm) = 8.41 (s, 1H), 7.90 (dd, 1H, J = 8.8 Hz, 2.0 Hz), 7.75 (d, 1H, J = 8.8 Hz), 7.57 (d, 1H, J = 8.8 Hz), 7.10 (d, 1H, J = 8.8 Hz), 6.83 (d, 1H, J = 2.0 Hz), 3.93 (s, 3H), 3.50 (q, 4H, J = 7.2 Hz), 1.24 (t, 6H, J = 7.2 Hz). HR-ESI-MS: m/z [$M + H$] calculated for $C_{16}H_{20}NO_2$, 258.1494; found, 258.1482.

Synthesis of 9: To a three-necked flask was added compound **5** (118 mg, 0.5 mmol) in 5 mL anhydrous THF. The solution was purged with N_2 for 10 min, and then NaH (57-63% oil dispersion, 200 mg, 5.0 mmol) was added. The resulting mixture was stirred for 30 min under N_2 at 65 °C, followed by the addition of compound **8** (130 mg, 0.5 mmol) in 5 mL THF via syringe pump over the course of 30 min. The reaction mixture was stirred for 24 hours at 65 °C under N_2 protection. After cooling to room temperature, the reaction was quenched by addition of water carefully in an ice bath. The pH was adjusted to 3 with HCl (aq). THF was removed under reduced pressure, and the aqueous suspension was extracted with dichloromethane. The combined organic phase was dried over anhydrous Na_2SO_4 , and concentrated under reduced pressure. The crude product was purified by column chromatography (silica gel, 50:1 to 10:1 v/v, petroleum ether/ethyl acetate) to afford product **9** as yellow solid (124 mg, 54%). 1H NMR (400 MHz, $CDCl_3$): δ (ppm) = 17.50 (s, 1H), 8.79 (s, 1H), 8.40 (s, 1H), 8.19 (d, 1H, J = 8.0 Hz), 8.13 (dd, 1H, J = 8.4 Hz, 1.6 Hz), 7.92 (dd, 1H, J = 8.4 Hz, 1.6 Hz), 7.80 (d, 1H, J = 8.0 Hz), 7.50 (d, 1H, J = 8.0 Hz), 7.40 (d, 2H, J = 8.4 Hz), 7.30 (d, 1H, J = 9.2 Hz), 7.10 (dd, 1H, J = 9.2 Hz, 2.4 Hz), 7.05 (s, 1H), 6.84 (d, 1H, J = 2.4 Hz), 4.33 (q, 2H, J = 7.2 Hz), 3.46 (q, 4H, J = 7.2 Hz), 1.45 (t, 3H, J = 7.2 Hz), 1.24 (t, 6H, J = 7.2 Hz). HR-ESI-MS: m/z [$M + H$] calculated for $C_{31}H_{31}N_2O_2$, 463.2386; found, 463.2370.

Synthesis of BF₂cna: To a solution of compound **9** (100 mg, 0.2 mmol) in 5 mL CH_2Cl_2 was added Et_3N (100 μ L, 0.7 mmol). The resulting solution was stirred for 10 min at room temperature, followed by the addition of BF_3/Et_2O (90 μ L, 0.7 mmol). The solution was stirred for another 2 hours in the dark. Water was added to the solution, and the organic layers was collected, washed with water, dried over anhydrous Na_2SO_4 , and concentrated

under reduced pressure. The crude product was purified by column chromatography (silica gel, 1:1 v/v, petroleum ether/dichloromethane) to afford product **BF₂cna** as purple solid (88 mg, 82%). ¹H NMR (400 MHz, DMSO-d₆): δ (ppm) = 8.31 (s, 1H), 8.85 (s, 1H), 8.48 (dd, 1H, *J* = 1.6 Hz, 8.8 Hz), 8.43 (d, 1H, *J* = 8.0 Hz), 8.21 (dd, 1H, *J* = 1.6 Hz, 8.8 Hz), 8.02 (d, 1H, *J* = 8.8 Hz), 7.97 (s, 1H), 7.87 (d, 1H, *J* = 8.8 Hz), 7.77 (q, 2H, *J* = 8.8 Hz), 7.60 (t, 1H, *J* = 7.6 Hz), 7.40 (t, 1H, *J* = 7.6 Hz), 7.30 (dd, 1H, *J* = 2.4 Hz, 9.2 Hz), 7.03 (s, 1H), 4.57 (q, 2H, *J* = 7.2 Hz), 3.56 (q, 4H, *J* = 7.2 Hz), 1.22 (t, 9H, *J* = 7.2 Hz). ¹³C NMR (100 MHz, DMSO-d₆) = 179.711, 179.00, 148.75, 143.63, 140.46, 138.92, 131.82, 131.52, 127.04, 126.77, 126.10, 124.37, 124.30, 123.29, 122.98, 122.88, 122.42, 122.11, 121.116, 120.53, 116.35, 110.13, 109.84, 103.93, 92.42, 44.03, 37.52, 13.77, 12.55. HR-ESI-MS: *m/z* [M + H] calculated for C₃₁H₃₀BF₂N₂O₂, 511.2368; found, 511.2354.

Synthesis of **11**^[3]: To a thick-wall flask was added compound **10** (1000 mg, 5.0 mmol) and 100 mL 36% HCl aqueous solution. The reaction mixture was refluxed overnight. After cooling to room temperature, the resulting mixture was filtered through Buchner funnel to obtain the product **11** as a light-yellow solid (700 mg, 75%). ¹H NMR (400 MHz, DMSO-d₆): δ (ppm) = 10.20 (s, 1H), 8.54 (s, 1H), 7.98 (d, 1H, *J* = 9.6 Hz), 7.88 (d, 1H, *J* = 8.8 Hz), 7.76 (d, 1H, *J* = 8.8 Hz), 7.19 (d, 2H, *J* = 6.8 Hz), 2.65 (s, 3H). HR-ESI-MS: *m/z* [M + H] calculated for C₁₂H₁₁O₂, 187.0759; found, 187.0752.

Synthesis of **12**:

Step 1:

Compound **11** (1000 mg, 5.38 mmol), Na₂S₂O₅ (3500 mg, 20.0 mmol) and 25% Ammonium Hydroxide (40 mL) were added to a hydrothermal autoclave, and reacted at 150 °C for 48 hours. The intermediate solid product 1-(6-Aminonaphthalen-2-yl)ethanone was obtained by filtration through Buchner funnel, washed with water twice, and dried in vacuum drying oven overnight.

Step 2:

To a high-pressure flask was added 5.0 mL DMF solution containing 1-(6-Aminonaphthalen-2-yl)ethanone (500 mg, 2.7 mmol), ethyl bromide (2.0 mL, 26.0 mmol) and isopropamide (1.0 mL, 6.0 mmol). The flask was sealed and heated under 80 °C for about 20 hours. After cooling to room temperature, the reaction solution was poured into 50 mL water and extracted with dichloromethane (20 mL × 5). The organic phase was dried over anhydrous Na₂SO₄, and concentrated under reduced pressure. The crude product was purified by column chromatography (silica gel, 4:1 v/v, petroleum ether/ethyl acetate) to afford the product **12** as white solid (395 mg, 61%). ¹H NMR (400 MHz, CDCl₃): δ (ppm) = 8.28 (s, 1H), 7.90 (dd, 1H, *J* = 1.6 Hz, 8.8 Hz), 7.76 (d, 1H, *J* = 8.8 Hz), 7.57 (d, 1H, *J* = 8.8 Hz), 7.10 (dd, 1H, *J* = 2.4 Hz), 6.20 (d, 1H, *J* = 2.4 Hz), 3.50 (q, 4H, *J* = 7.2 Hz), 2.66 (s, 3H), 1.24 (t, 6H, *J* = 7.2 Hz). HR-ESI-MS: *m/z* [M + H] calculated for C₁₆H₂₀NO, 242.1545; found, 242.1541.

Synthesis of **13**: To a three-necked flask was added compound **12** (190 mg, 0.95 mmol) in 5 mL anhydrous THF. The solution was purged with N₂ for 10 min, and then added NaH (57-63% oil dispersion, 200 mg, 5.0 mmol). The resulting mixture was stirred 30 min under

N₂ at 65 °C, followed by addition of compound **8** (244 mg, 0.95 mmol) in 5 mL THF via injection pump over the course of 30 minutes. The reaction mixture was stirred for 24 hours at 65 °C under N₂ protection. After cooling to room temperature, the reaction was quenched by addition of water carefully in an ice bath. The pH was adjusted to 3 with HCl (aq). THF was removed under reduced pressure and the residue was extracted with dichloromethane. The combined organic phase was dried over anhydrous Na₂SO₄, and concentrated under reduced pressure. The crude product was purified by column chromatography (silica gel, 10:1 v/v, petroleum ether/ethyl acetate) to afford product **13** as orange solid (198 mg, 45%). ¹H NMR (400 MHz, CDCl₃): δ (ppm) = 17.36 (s, 1H), 8.42 (s, 2H), 7.94 (d, 2H, *J* = 8.8 Hz), 7.81 (d, 2H, *J* = 9.2 Hz), 7.64 (d, 2H, *J* = 8.8 Hz), 7.12 (d, 2H, *J* = 8.8 Hz), 7.05 (s, 1H), 6.86 (s, 2H), 3.50 (q, 8H, *J* = 7.2 Hz), 1.25 (t, 12H, *J* = 7.2 Hz). HR-ESI-MS: *m/z* [M + H] calculated for C₃₁H₃₅N₂O₂, 467.2699; found, 467.2691.

Synthesis of **BF₂dan**: To a solution of compound **13** (230 mg, 0.5 mmol) in 10 mL CH₂Cl₂ was added Et₃N (210 μL, 1.5 mmol). After stirring for 10 min at room temperature, BF₃/Et₂O (200 μL, 1.5 mmol) was added. The solution was stirred for another 2 hours in the dark. Water was added to the solution, and the organic layers was collected, washed with water, dried over anhydrous Na₂SO₄, and concentrated under reduced pressure. The crude product was purified by column chromatography (silica gel, 1:1 v/v, petroleum ether/dichloromethane) to afford product **BF₂dan** as scarlet solid (219 mg, 85%). ¹H NMR (400 MHz, CDCl₃): δ (ppm) = 8.61 (d, 2H, *J* = 1.6 Hz), 7.96 (dd, 2H, *J* = 1.6 Hz, 8.8 Hz), 7.83 (d, 2H, *J* = 9.2 Hz), 7.61 (d, 2H, *J* = 8.8 Hz), 7.27 (s, 1H), 7.13 (dd, 2H, *J* = 2.4 Hz, 9.2 Hz), 6.84 (dd, 2H, *J* = 2.4 Hz, 8.4 Hz), 3.50 (q, 8H, *J* = 7.2 Hz), 1.28 (t, 12H, *J* = 7.2 Hz). ¹³C NMR (100 MHz, DMSO-*d*₆): δ (ppm) = 188.45, 148.75, 138.87, 131.80, 129.63, 126.10, 124.40, 123.34, 116.37, 103.94, 98.44, 44.04, 12.57. HR-ESI-MS: *m/z* [M + H] calculated for C₃₁H₃₄BF₂N₂O₂, 515.2681; found, 515.2670.

(2) Preparation of nanocrystals and their reproducibility

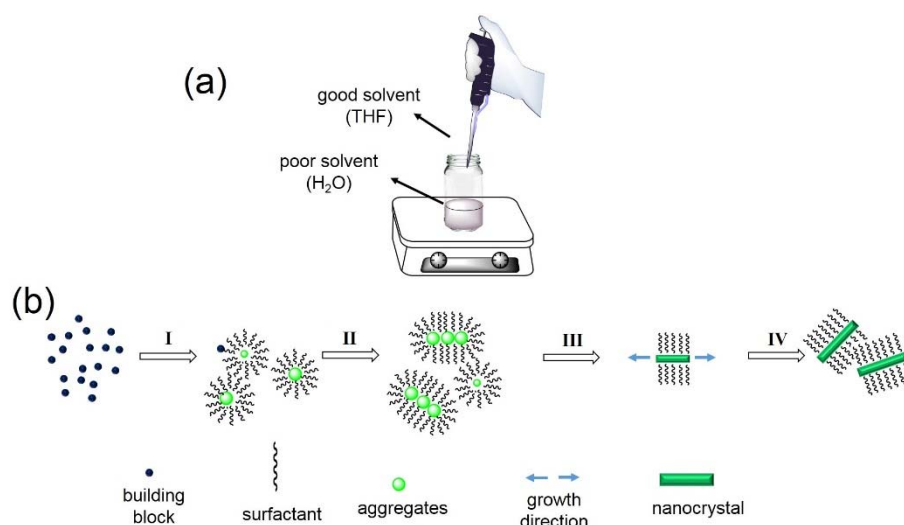


Figure S1. (a) Schematic drawing of the preparation of the nanocrystals; (b) schematic illustration representing formation of nanocrystals in the presence of surfactant: stage I,

formation of molecular aggregates; stage II, the fusion of aggregates; stages III and IV, organization and growth of nanocrystals.

In a typical preparation of the nanocrystals, a solution of BF₂bcz (1.0 mM) with different ratios of acceptor BF₂cna or BF₂dan (0 - 0.1 mol%) in THF (good solvent, 1.0 mL) was injected into 5.0 mL SDS (2.0 mg/mL) aqueous solution (poor solvent for building blocks) with vigorous stirring. After stirring for 3 min, the sample was left undisturbed for about 20 hours for stabilization. During the aging time, the vial was kept sealed. Surfactant played an important role in the formation of nanocrystals. Upon addition of the THF solution of building blocks to water containing surfactant, the solubility of the building blocks significantly decreased and the aggregates covered with surfactant formed immediately. The aggregates slowly assembled into nanocrystals in the mixed solvent with the help of surfactant. The surfactant stabilized the aggregates and induced the growth of the nanocrystals. The surfactant could selectively adhere on a certain facet and slow down the grow rate of that facet compared with the others, leading to the formation of nanorods in our systems.^[4]

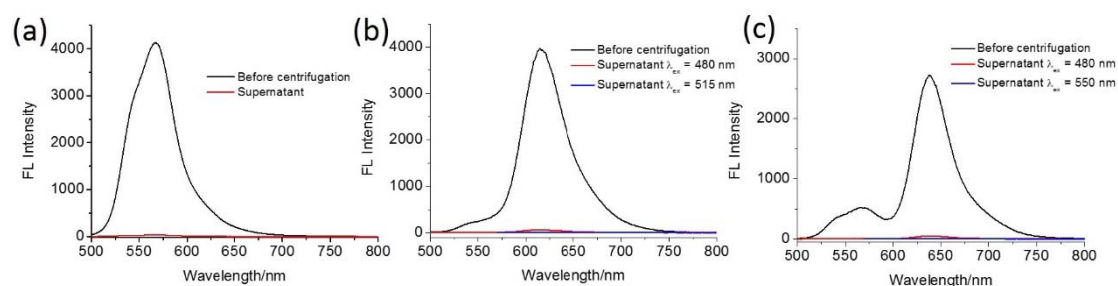


Figure S2. The emission spectra of the aqueous dispersions of nanocrystals before (black line) and the supernatant (red and blue line) after ultrasound/centrifugation of the as prepared samples. (a) BF₂bcz nanocrystals, (b) 0.05 mol% BF₂cna doped nanocrystals, (c) 0.05 mol% BF₂dan doped nanocrystals. $\lambda_{\text{ex}} = 480$ nm, excitation donors; $\lambda_{\text{ex}} = 515$ nm and 550 nm, direct excitation acceptor BF₂cna and BF₂dan respectively.

To prove that molar ratio in nanocrystals is consistent with that in solution, we separated the supernatant from the pristine preparing mixture of co-nanocrystals by centrifugal process. The supernatant showed negligible fluorescence, indicating the building blocks completely assembled into nanocrystals since the donor and acceptor molecules in our system show strong fluorescence both in solution and in solid state. From this observation, we speculate that the molar ratio relevant to solution persist in the nanocrystals.

The SEM images showed uniform morphology and size for each batch of samples. And the characterization of the nanocrystals including the XRD performance, spectral measurement for the samples with different doping ratios, the lifetime determination and the fluorescence microscopy images, have repeated twice or three times, and showed good reproducibility.

If the SDS solution was replaced by sodium dodecyl benzene sulfonate (2 mg/mL) or hexadecyl trimethyl ammonium bromide (0.5 mg/mL) solution, and other conditions kept the same, nanocrystals were also obtained with uniform size and shape (Figure S4).

3. Characterization of nanocrystals and spectroscopies of chromophores and nanocrystals

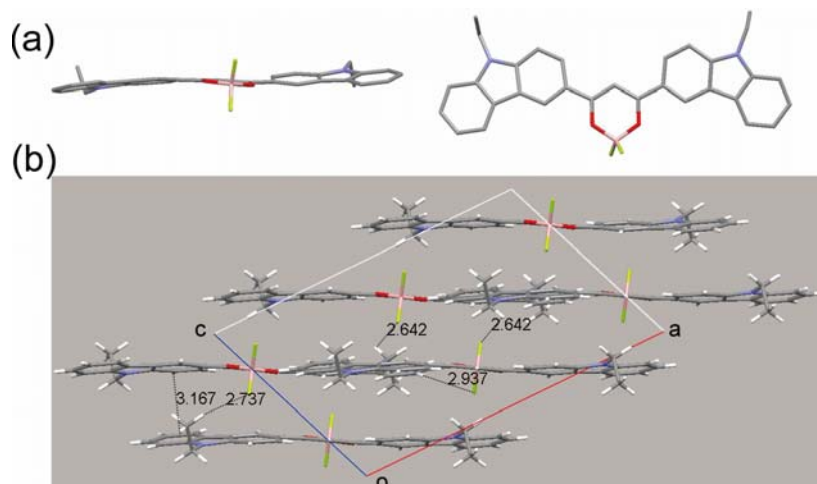


Figure S3. (a) Capped sticks crystal structures of BF₂bcz in the side view and front view, respectively. (b) Intermolecular CH.....F and CH..... π interactions in the unit cell of the BF₂bcz crystal viewed along the b direction.

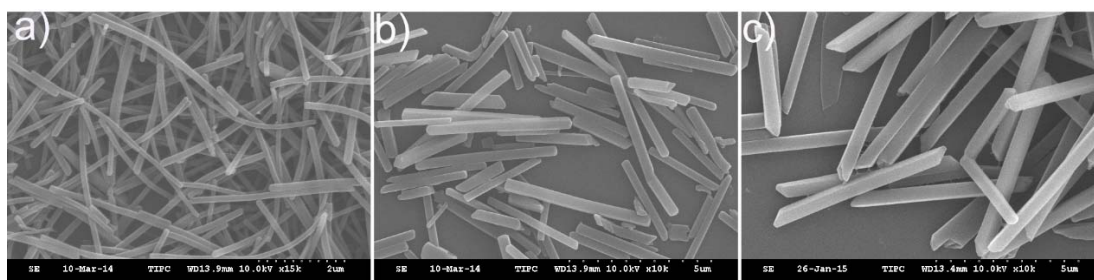


Figure S4. The SEM images of BF₂bcz nanocrystals prepared in water with CTAB (a), SDBS (b) and SDS (c) as the surfactant.

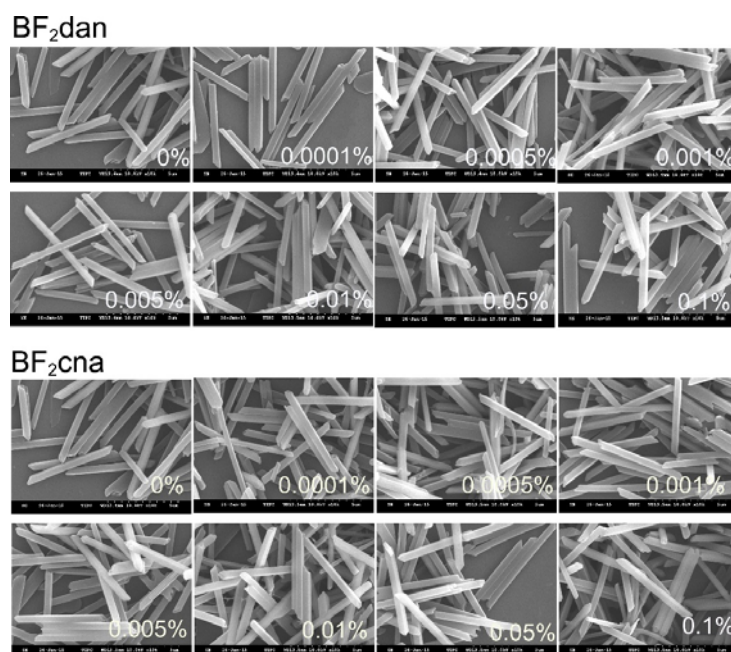


Figure S5. The SEM images of BF₂bcz nanocrystals doped with different ratios of BF₂dan (top) and BF₂cna (below).

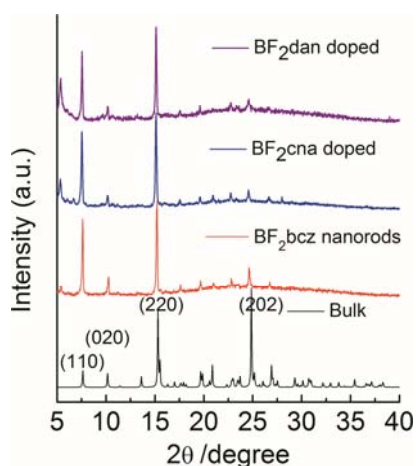


Figure S6. X-ray diffraction (XRD) patterns of bulk crystal of BF₂bcz, BF₂bcz nanocrystals and the nanocrystals doped with 0.1 mol% BF₂dan or BF₂cna.

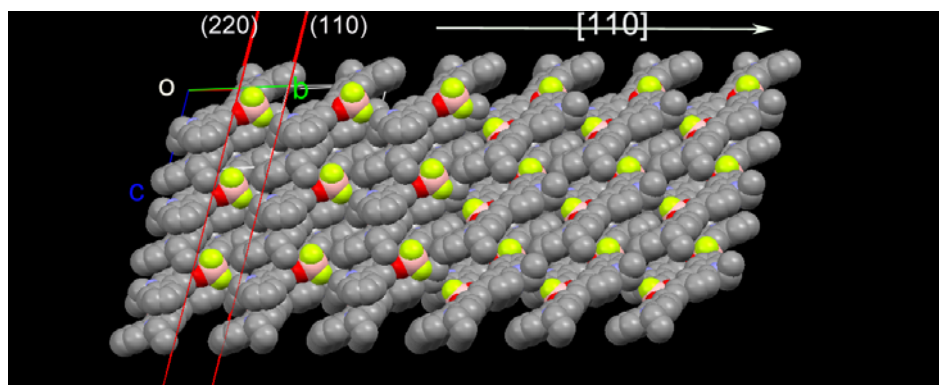


Figure S7. The molecular stacking of BF₂bcz in the nanocrystals along [110] direction.

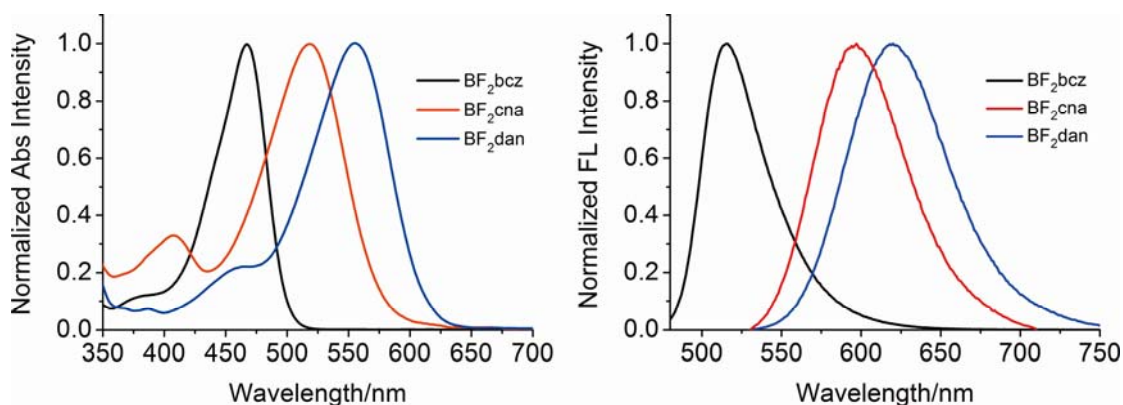


Figure S8. The normalized absorption (left) and emission spectra (right) of BF₂bcz, BF₂cna and BF₂dan in CH₂Cl₂ at the concentration of 5 μ M. The BF₂bcz, BF₂cna and BF₂dan are typical D-A-D type fluorophore, with the difluoroboron moiety acting as the electron acceptor and the carbazole or amino-naphthalene units serving as the electron donor. Their excited states showed intramolecular charge transfer (ICT) character. Variation of the electron donating group affect significantly to their photophysical properties. The large red-shift for the spectra of BF₂dan compared with that of BF₂cna ascribed to the more predominant electro-donating capability of the amino-naphthalene units than that of carbazole units.

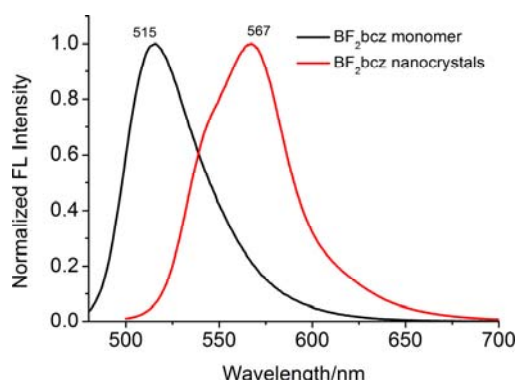


Figure S9. The normalized emission spectra of aqueous dispersion of BF₂bcz nanocrystals and BF₂bcz monomer in CH₂Cl₂.

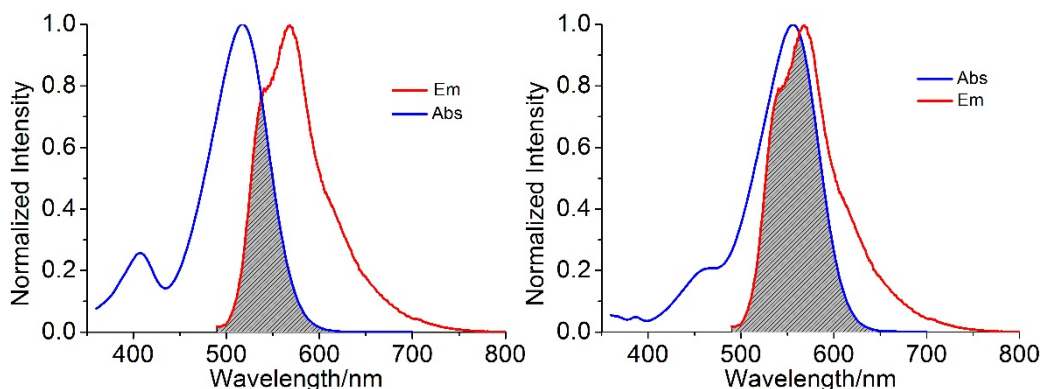


Figure S10. The spectral overlap of the emission of aqueous dispersion of BF₂bcz nanocrystals and the absorption of BF₂cna (left) and BF₂dan (right) in CH₂Cl₂.

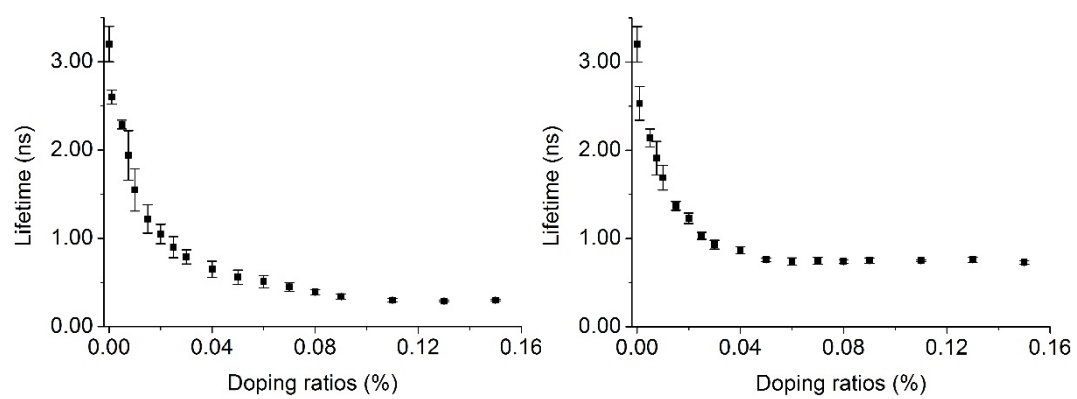


Figure S11. The fluorescence lifetime of BF₂bcz nanocrystals with different doping ratios of BF₂cna (left) and BF₂dan (right).

Table S1. The fluorescence decay lifetimes of nanocrystals with different doping ratios

	Acceptors	
Doping ratio (mol%)	BF ₂ cna	BF ₂ dan
0	$\alpha_1 = 0.38 \pm 0.07, \tau_1 = 3.25 \pm 0.20; \alpha_2 = 0.62 \pm 0.07, \tau_2 = 5.50 \pm 0.14$	
0.001	$\alpha_1 = 0.32 \pm 0.06, \tau_1 = 2.50 \pm 0.18$ $\alpha_2 = 0.68 \pm 0.06, \tau_2 = 5.35 \pm 0.12$	$\alpha_1 = 0.32 \pm 0.01, \tau_1 = 2.53 \pm 0.19$ $\alpha_2 = 0.68 \pm 0.01, \tau_2 = 5.16 \pm 0.12$
0.005	$\alpha_1 = 0.77 \pm 0.05, \tau_1 = 2.29 \pm 0.05$ $\alpha_2 = 0.23 \pm 0.05, \tau_2 = 4.93 \pm 0.07$	$\alpha_1 = 0.59 \pm 0.08, \tau_1 = 2.14 \pm 0.10$ $\alpha_2 = 0.41 \pm 0.08, \tau_2 = 4.77 \pm 0.34$
0.0075	$\alpha_1 = 0.85 \pm 0.06, \tau_1 = 1.94 \pm 0.28$ $\alpha_2 = 0.15 \pm 0.06, \tau_2 = 5.00 \pm 0.04$	$\alpha_1 = 0.65 \pm 0.04, \tau_1 = 1.91 \pm 0.19$ $\alpha_2 = 0.35 \pm 0.04, \tau_2 = 4.40 \pm 0.08$
0.01	$\alpha_1 = 0.90 \pm 0.02, \tau_1 = 1.55 \pm 0.24$ $\alpha_2 = 0.10 \pm 0.02, \tau_2 = 4.86 \pm 0.14$	$\alpha_1 = 0.70 \pm 0.03, \tau_1 = 1.69 \pm 0.14$ $\alpha_2 = 0.30 \pm 0.03, \tau_2 = 4.61 \pm 0.22$
0.015	$\alpha_1 = 0.93 \pm 0.02, \tau_1 = 1.22 \pm 0.16$ $\alpha_2 = 0.07 \pm 0.02, \tau_2 = 5.09 \pm 0.11$	$\alpha_1 = 0.75 \pm 0.02, \tau_1 = 1.37 \pm 0.05$ $\alpha_2 = 0.25 \pm 0.02, \tau_2 = 4.26 \pm 0.11$
0.02	$\alpha_1 = 0.95 \pm 0.01, \tau_1 = 1.05 \pm 0.11$ $\alpha_2 = 0.05 \pm 0.01, \tau_2 = 4.76 \pm 0.14$	$\alpha_1 = 0.78 \pm 0.01, \tau_1 = 1.23 \pm 0.06$ $\alpha_2 = 0.22 \pm 0.01, \tau_2 = 4.45 \pm 0.18$
0.025	$\alpha_1 = 0.96 \pm 0.01, \tau_1 = 0.87 \pm 0.12$ $\alpha_2 = 0.04 \pm 0.01, \tau_2 = 4.95 \pm 0.17$	$\alpha_1 = 0.77 \pm 0.02, \tau_1 = 1.03 \pm 0.04$ $\alpha_2 = 0.23 \pm 0.02, \tau_2 = 4.15 \pm 0.34$
0.03	$\alpha_1 = 0.97 \pm 0.01, \tau_1 = 0.79 \pm 0.08$ $\alpha_2 = 0.03 \pm 0.01, \tau_2 = 4.92 \pm 0.19$	$\alpha_1 = 0.80 \pm 0.01, \tau_1 = 0.93 \pm 0.05$ $\alpha_2 = 0.20 \pm 0.01, \tau_2 = 3.55 \pm 0.04$
0.04	$\alpha_1 = 0.97 \pm 0.01, \tau_1 = 0.65 \pm 0.09$ $\alpha_2 = 0.03 \pm 0.01, \tau_2 = 5.13 \pm 0.21$	$\alpha_1 = 0.80 \pm 0.01, \tau_1 = 0.87 \pm 0.04$ $\alpha_2 = 0.20 \pm 0.01, \tau_2 = 3.69 \pm 0.10$
0.05	$\alpha_1 = 0.98 \pm 0.01, \tau_1 = 0.56 \pm 0.08$ $\alpha_2 = 0.02 \pm 0.01, \tau_2 = 5.38 \pm 0.20$	$\alpha_1 = 0.81 \pm 0.01, \tau_1 = 0.76 \pm 0.02$ $\alpha_2 = 0.19 \pm 0.01, \tau_2 = 3.29 \pm 0.07$
0.06	$\alpha_1 = 0.98 \pm 0.01, \tau_1 = 0.51 \pm 0.07$ $\alpha_2 = 0.02 \pm 0.01, \tau_2 = 4.91 \pm 0.18$	$\alpha_1 = 0.81 \pm 0.02, \tau_1 = 0.74 \pm 0.04$ $\alpha_2 = 0.19 \pm 0.02, \tau_2 = 3.39 \pm 0.08$
0.07	$\alpha_1 = 0.98 \pm 0.01, \tau_1 = 0.45 \pm 0.05$ $\alpha_2 = 0.02 \pm 0.01, \tau_2 = 5.27 \pm 0.23$	$\alpha_1 = 0.81 \pm 0.03, \tau_1 = 0.75 \pm 0.01$ $\alpha_2 = 0.19 \pm 0.03, \tau_2 = 3.51 \pm 0.05$
0.08	$\alpha_1 = 0.98 \pm 0.01, \tau_1 = 0.39 \pm 0.03$ $\alpha_2 = 0.02 \pm 0.01, \tau_2 = 5.26 \pm 0.13$	$\alpha_1 = 0.80 \pm 0.01, \tau_1 = 0.74 \pm 0.02$ $\alpha_2 = 0.20 \pm 0.01, \tau_2 = 3.31 \pm 0.02$
0.09	$\alpha_1 = 0.99 \pm 0.01, \tau_1 = 0.34 \pm 0.03$ $\alpha_2 = 0.01 \pm 0.01, \tau_2 = 5.46 \pm 0.29$	$\alpha_1 = 0.80 \pm 0.01, \tau_1 = 0.75 \pm 0.03$ $\alpha_2 = 0.20 \pm 0.01, \tau_2 = 3.65 \pm 0.07$
0.11	$\alpha_1 = 0.98 \pm 0.01, \tau_1 = 0.30 \pm 0.02$ $\alpha_2 = 0.02 \pm 0.01, \tau_2 = 5.70 \pm 0.20$	$\alpha_1 = 0.79 \pm 0.02, \tau_1 = 0.75 \pm 0.01$ $\alpha_2 = 0.21 \pm 0.02, \tau_2 = 3.11 \pm 0.04$
0.13	$\alpha_1 = 0.99 \pm 0.01, \tau_1 = 0.29 \pm 0.01$ $\alpha_2 = 0.01 \pm 0.01, \tau_2 = 5.83 \pm 0.22$	$\alpha_1 = 0.85 \pm 0.02, \tau_1 = 0.76 \pm 0.03$ $\alpha_2 = 0.15 \pm 0.02, \tau_2 = 2.38 \pm 0.04$
0.15	$\alpha_1 = 0.97 \pm 0.01, \tau_1 = 0.30 \pm 0.02$ $\alpha_2 = 0.03 \pm 0.01, \tau_2 = 6.09 \pm 0.18$	$\alpha_1 = 0.82 \pm 0.02, \tau_1 = 0.73 \pm 0.02$ $\alpha_2 = 0.18 \pm 0.02, \tau_2 = 2.27 \pm 0.03$

α is fractional amplitude. τ is fluorescence lifetime in the unit of ns.

The fluorescence lifetime determination has been repeated for three times. The decay curves were well fitted by using a two-exponential function (see section 5, the screenshots

of lifetime decay profiles of each doping ratio, S28 – S31). The short component, whose values are sensitive to the concentrations of acceptors, represents the quenching of the excitons by the acceptors immobilized within the nanocrystals. While the long decay component, probably derives from the donor molecules located at the edge or the surface of nanocrystals, which is expected to be quenched less efficiently.

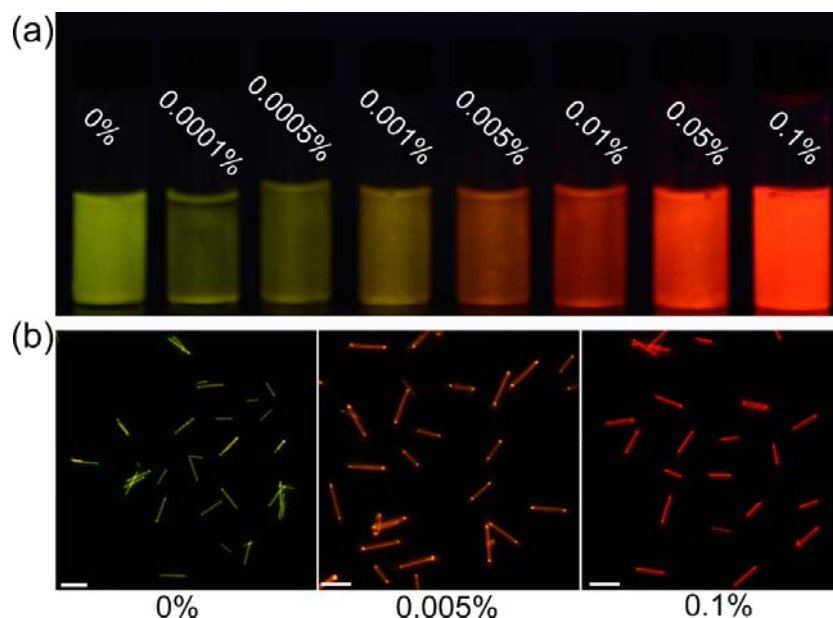


Figure S12. (a) The fluorescence images of the aqueous dispersions of nanocrystals doped with different amounts of BF₂cna. (b) The fluorescence microscopy images of nanocrystals with different amounts of BF₂cna. The scale bar is 5 μ m.

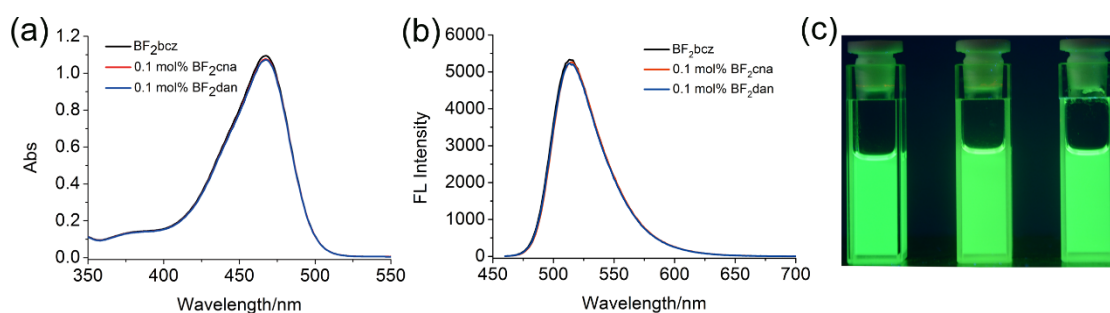


Figure S13. (a) and (b) the absorption and fluorescence spectra of BF₂bcz (1×10^{-5} M, black), BF₂cna/BF₂bcz (0.1 mol%, C(BF₂bcz) = 1×10^{-5} M, red) and BF₂dan/BF₂bcz (0.1 mol%, C(BF₂bcz) = 1×10^{-5} M, blue) in CH₂Cl₂. (c) The fluorescence photos of the BF₂bcz (1 mM, left), BF₂cna/BF₂bcz (0.1 mol%, C(BF₂bcz) = 1 mM, middle) and BF₂dan/BF₂bcz (0.1 mol%, C(BF₂bcz) = 1 mM, right) in CH₂Cl₂.

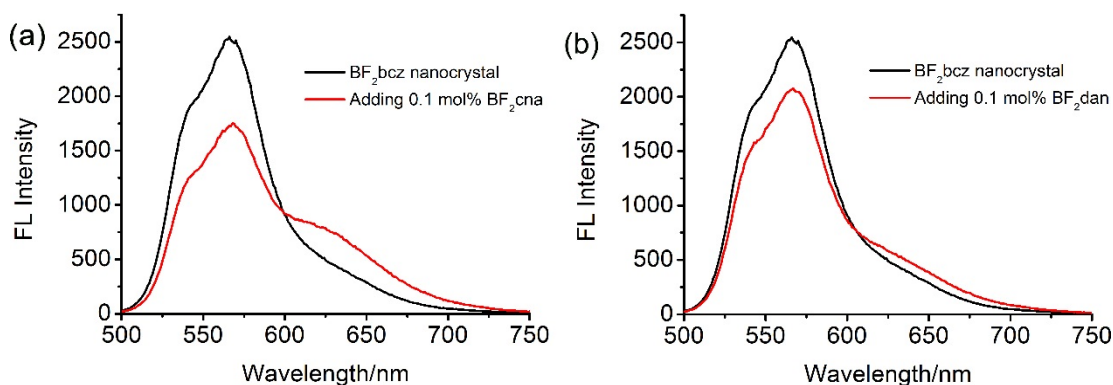


Figure S14. The emission spectra of BF₂bcz nanocrystal (black line) and the as-prepared nanocrystals subsequently by addition of 0.1 mol% BF₂cna (a, red line) and BF₂dan (b, red line).

To prove the feature that the acceptor co-crystallized with the donor, we performed a control experiment. We prepared the nanocrystals containing only donor molecules, followed by the addition of 0.1 mol% acceptors. The energy transfer was observed for the resulting aqueous dispersion of the nanocrystals, but the efficiency was much lower (less than 30%) than the co-crystal system (95%) at the identical condition. In such system, the acceptor molecules should be located on the surface of the nanocrystals rather than co-crystallized with donor, resulting in low energy transfer efficiency. This result indicated that the efficient energy transfer could not be obtained without the well-defined orientation and distance between the donors and acceptors. Therefore, the acceptors should be co-crystallized with donors, not just located on the surface of the nanocrystals, to ensure the occurrence of efficient energy transfer.

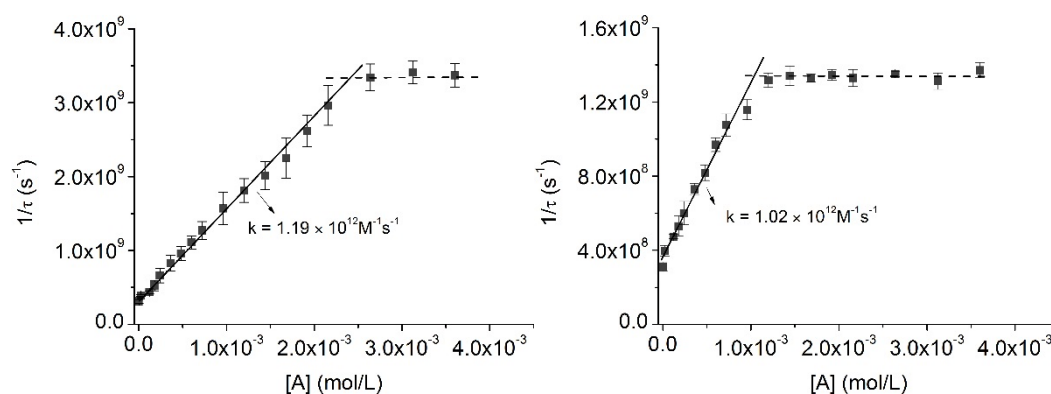
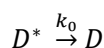
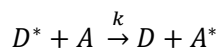


Figure S15. Plotting of the reciprocal lifetime of the BF₂bcz nanocrystals containing different concentrations of BF₂cna (left) and BF₂dan (right) monitored at 540 nm against the concentrations of the acceptors.

The acceptor molecules are immobilized within the crystal, and only the excitons are migratory. Thus we proposed the second-order rate equation to describe the quenching process of the excitons with the acceptors^[5]



Where D is the donor and A refers to the acceptor, “*” denotes the excited state.

The quenching rate equation can be written as

$$\frac{d[D^*]}{dt} = -k[D^*][A] - k_0[D^*]$$

Since the excitation power is very low in the single-photon counting fluorescence lifetime measurement, we can assume that $[A] \gg [D^*]$, and therefore $k' = k[A]$. Thus, we have

$$[D^*] \propto e^{-(k'+k_0)t} = e^{-\frac{1}{\tau}t}$$

i.e., the quenching of the excitons follows a monoexponential process, and the second-order rate constant can be derived by plotting $1/\tau$ against the doping concentration $[A]$ in a unit of M (the concentration was estimated by using the parameters of BF₂bcz crystal data), where k equals the slope, the intercept is k_0 which is the reciprocal of τ_0 (the intrinsic lifetime of the donor).

For both acceptors, the rate constant is in an order of $10^{12} \text{ M}^{-1}\text{s}^{-1}$, which is apparently larger than the diffusion limit for the bimolecular reaction in the solution.^[6] Therefore, the much larger second order rate can be ascribed to the favorable spatial orientation as well as a possible shorter mean average distance in contrast to those in the solution phase. Our result indicates that the excitonic energy migration rate within the nanocrystal would be much larger than that of the diffusion limit in solution.

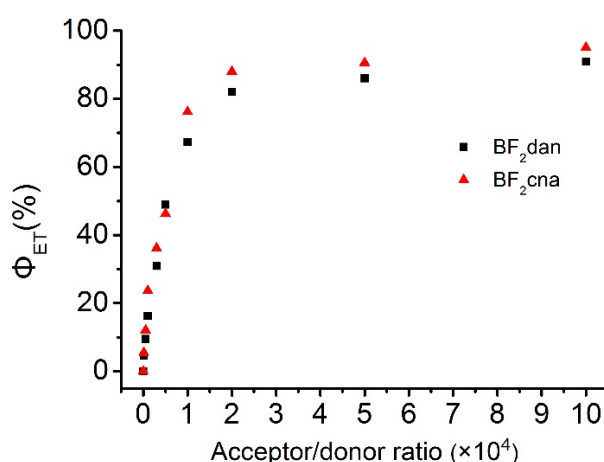


Figure S16. Energy transfer efficiency versus acceptor/donor ratios.

The exciton energy transfer is more efficient for the BF₂cna as acceptor than the BF₂dan as the acceptor. We speculated that the structural similarity plays important role for more efficient energy transfer for BF₂cna than for BF₂dan. The BF₂cna, containing a carbazole group, could easily co-assembly with the two-carbazole-containing donor BF₂bcz to form nanocrystals in which the BF₂cna molecules were dispersed uniformly. The BF₂dan (containing two naphthalene) probably is less favorable than BF₂cna to co-assembly with BF₂bcz. With the increasing the ratio of the acceptor to donor, BF₂dan molecules may not disperse uniformly in the nanocrystals, resulting in the less efficient energy transfer than co-nanocrystals of BF₂cna/BF₂bcz at the identical condition.

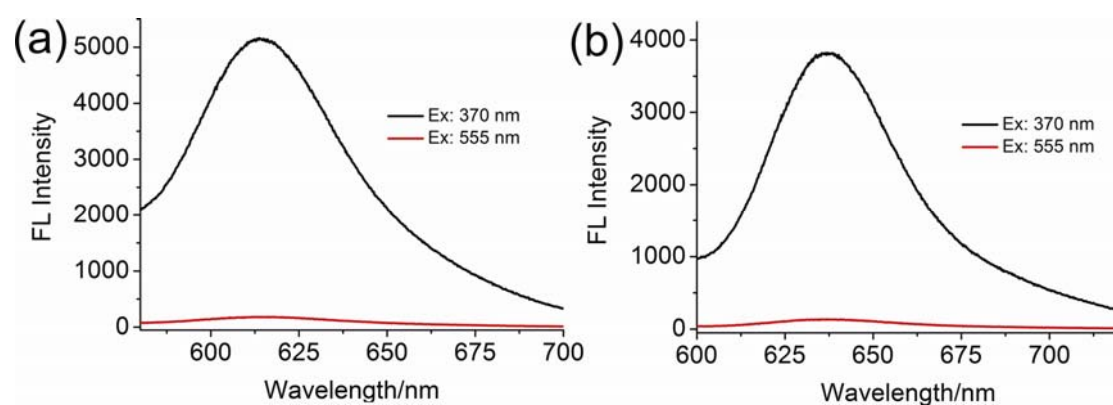


Figure S17. The emission spectra of BF₂cna/BF₂bcz (0.01 mol%, a) and BF₂dan/BF₂bcz (0.01 mol%, b) nanocrystals upon excitation of acceptor at 555 nm (red line) and excitation of donor at 370 nm (black line), respectively.

Table S2. Crystal data and structure refinement for BF₂bcz (CCDC 1042445)

Identification code	a	
Empirical formula	C ₃₂ H ₂₆ B Cl ₃ F ₂ N ₂ O ₂	
Formula weight	625.71	
Temperature	173.1500 K	
Wavelength	0.71073 Å	
Crystal system	Monoclinic	
Space group	C 1 2/c 1	
Unit cell dimensions	a = 16.633(3) Å	α = 90°.
	b = 17.400(4) Å	β = 111.47(3)°.
	c = 10.483(2) Å	γ = 90°.
Volume	2823.5(11) Å ³	
Z	4	
Density (calculated)	1.472 Mg/m ³	
Absorption coefficient	0.373 mm ⁻¹	
F(000)	1288	
Crystal size	0.52 x 0.15 x 0.15 mm ³	
Theta range for data collection	1.761 to 27.431°.	
Index ranges	-21 ≤ h ≤ 21, -22 ≤ k ≤ 22, -13 ≤ l ≤ 5	
Reflections collected	11420	
Independent reflections	3223 [R(int) = 0.0749]	
Completeness to theta = 26.000°	99.9 %	
Absorption correction	Semi-empirical from equivalents	
Max. and min. transmission	1.0000 and 0.6885	
Refinement method	Full-matrix least-squares on F ²	
Data / restraints / parameters	3223 / 26 / 217	
Goodness-of-fit on F ²	1.130	
Final R indices [I > 2σ(I)]	R1 = 0.0760, wR2 = 0.1835	
R indices (all data)	R1 = 0.0848, wR2 = 0.1895	
Extinction coefficient	n/a	
Largest diff. peak and hole	0.528 and -0.560 e.Å ⁻³	

4. The NMR and HR-ESI spectra of chromophores

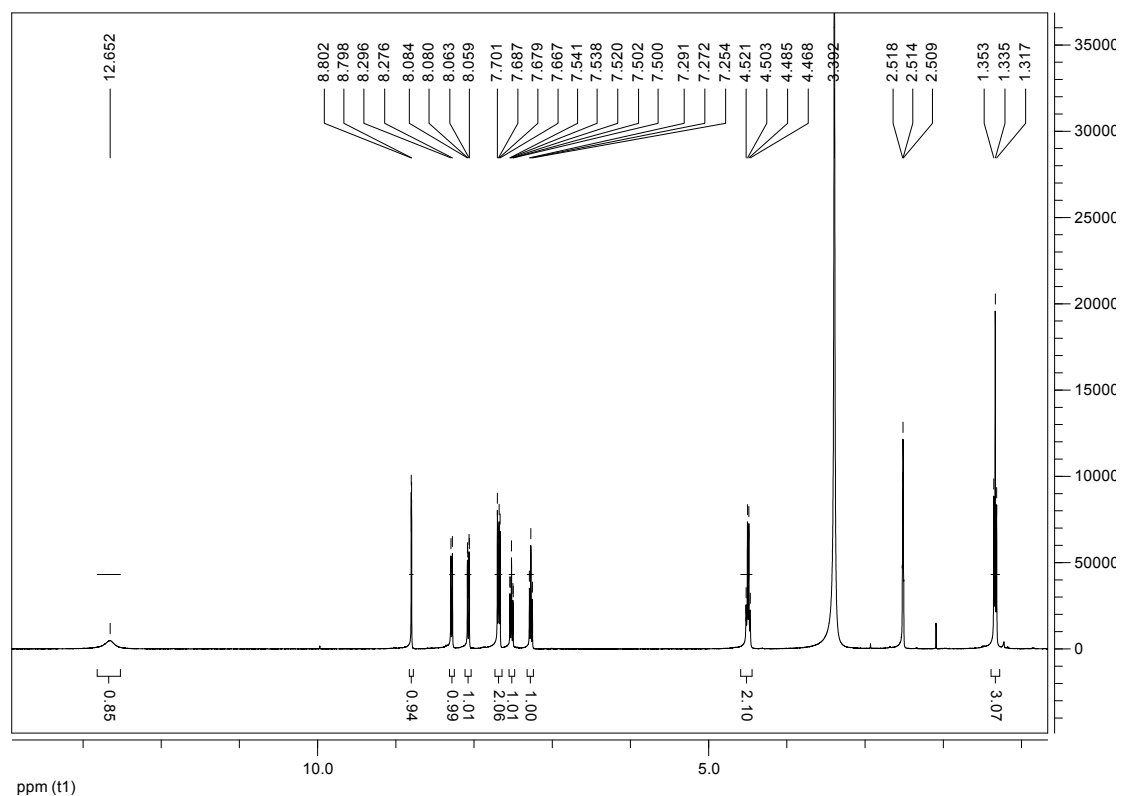


Figure S18. The ¹H NMR spectrum of **2** in DMSO-d₆.

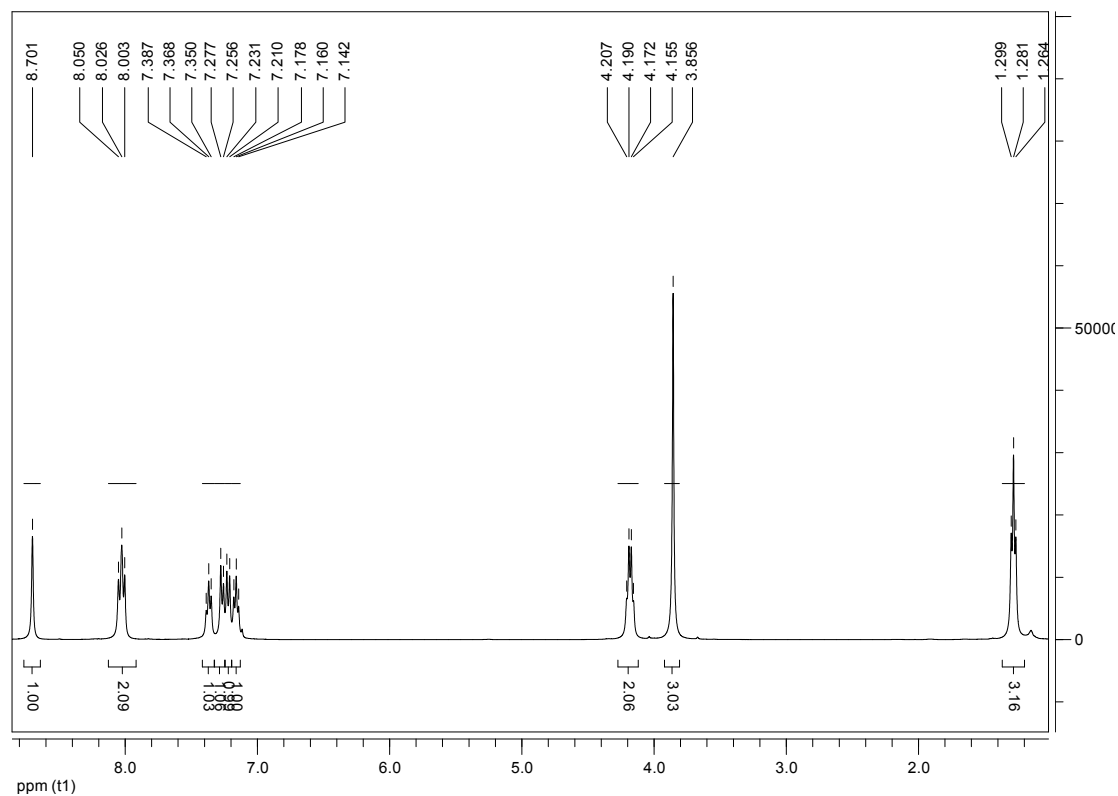


Figure S19. The ¹H NMR spectrum of **3** in CDCl₃.

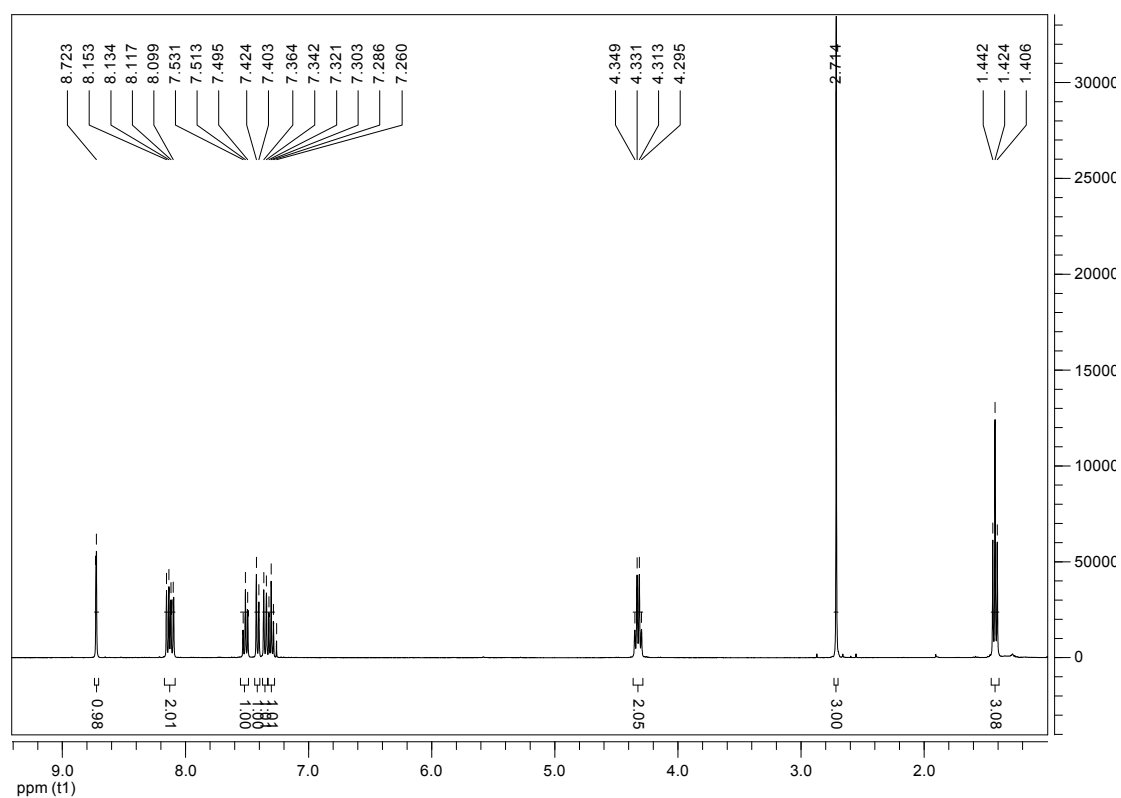


Figure S20. The ^1H NMR spectrum of **5** in CDCl_3 .

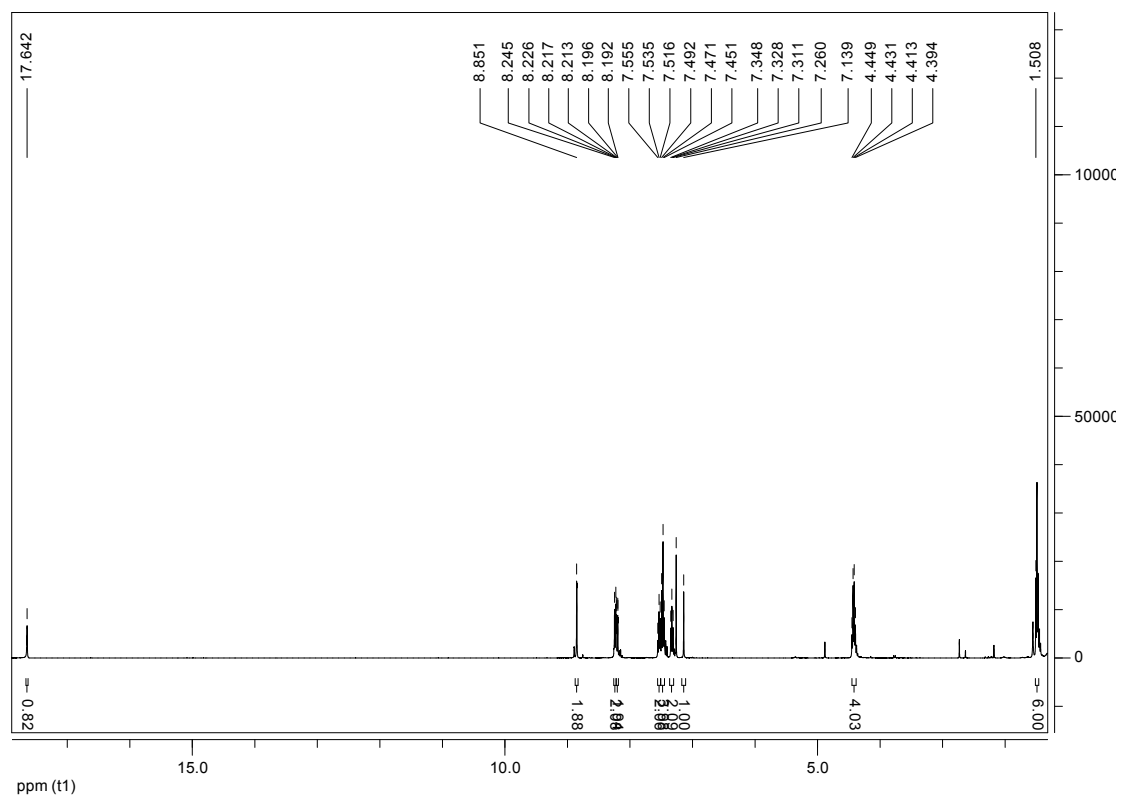


Figure S21. The ^1H NMR spectrum of **6** in CDCl_3 .

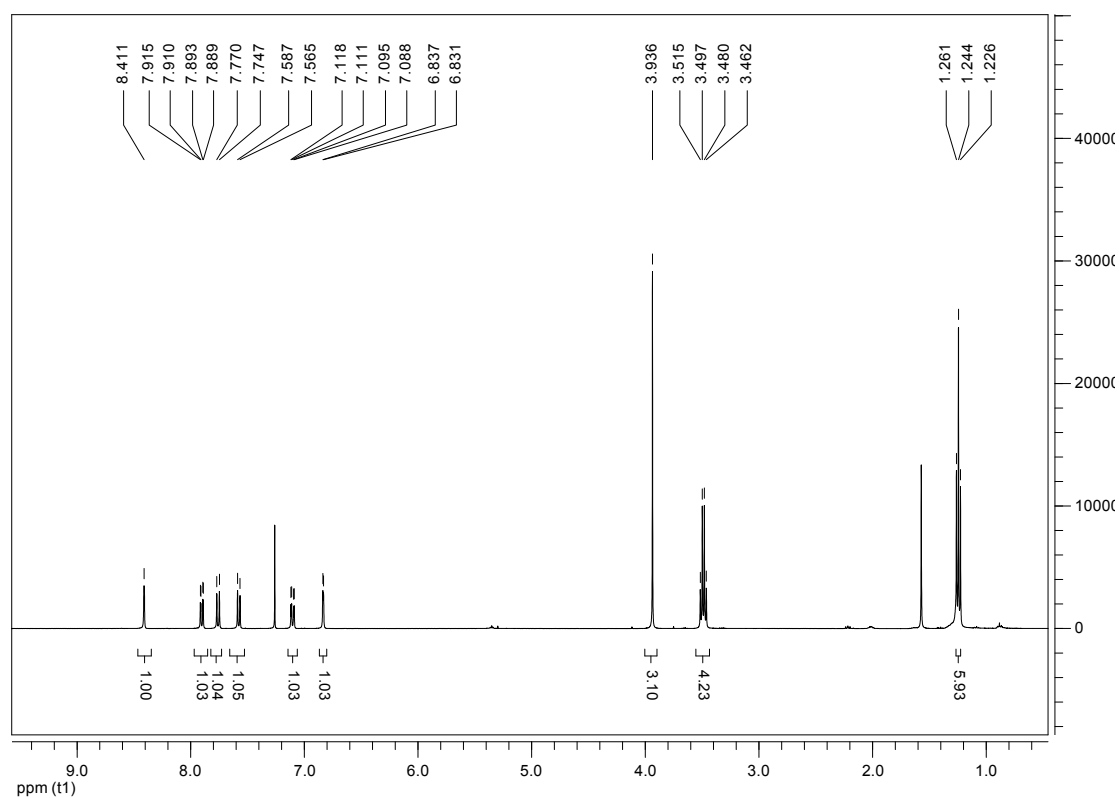


Figure S22. The ^1H NMR spectrum of **8** in CDCl_3 .

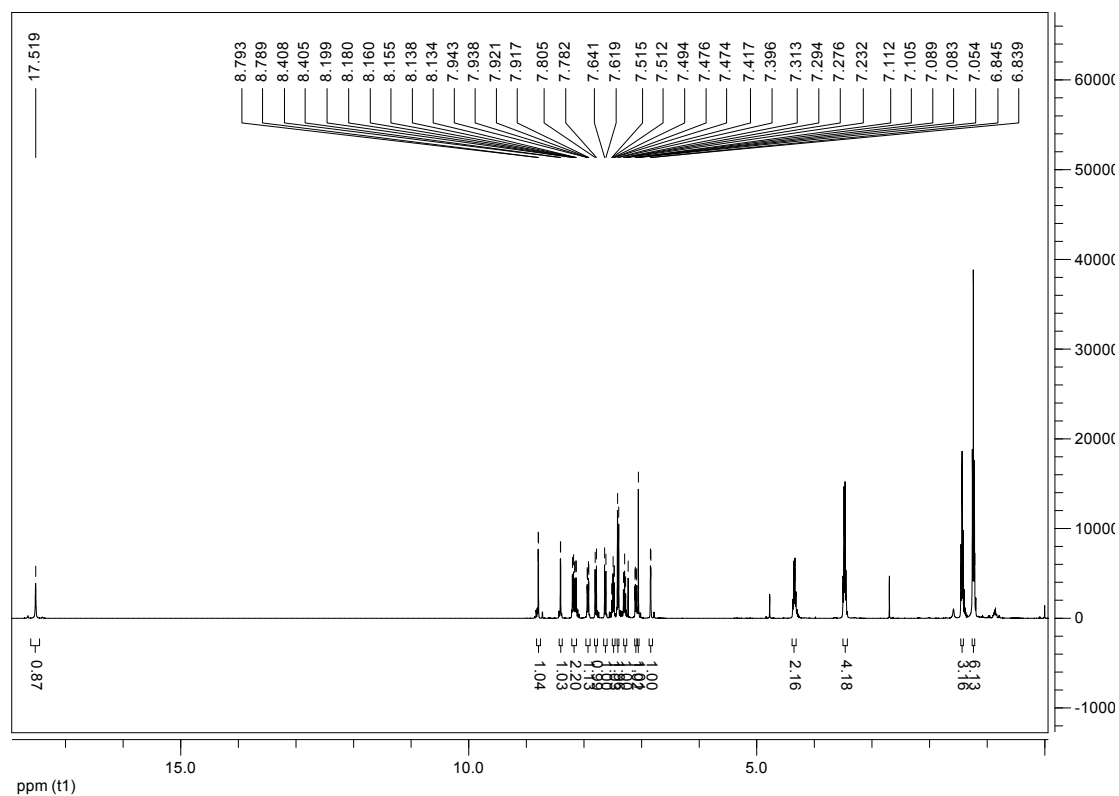


Figure S23. The ^1H NMR spectrum of **9** in CDCl_3 .

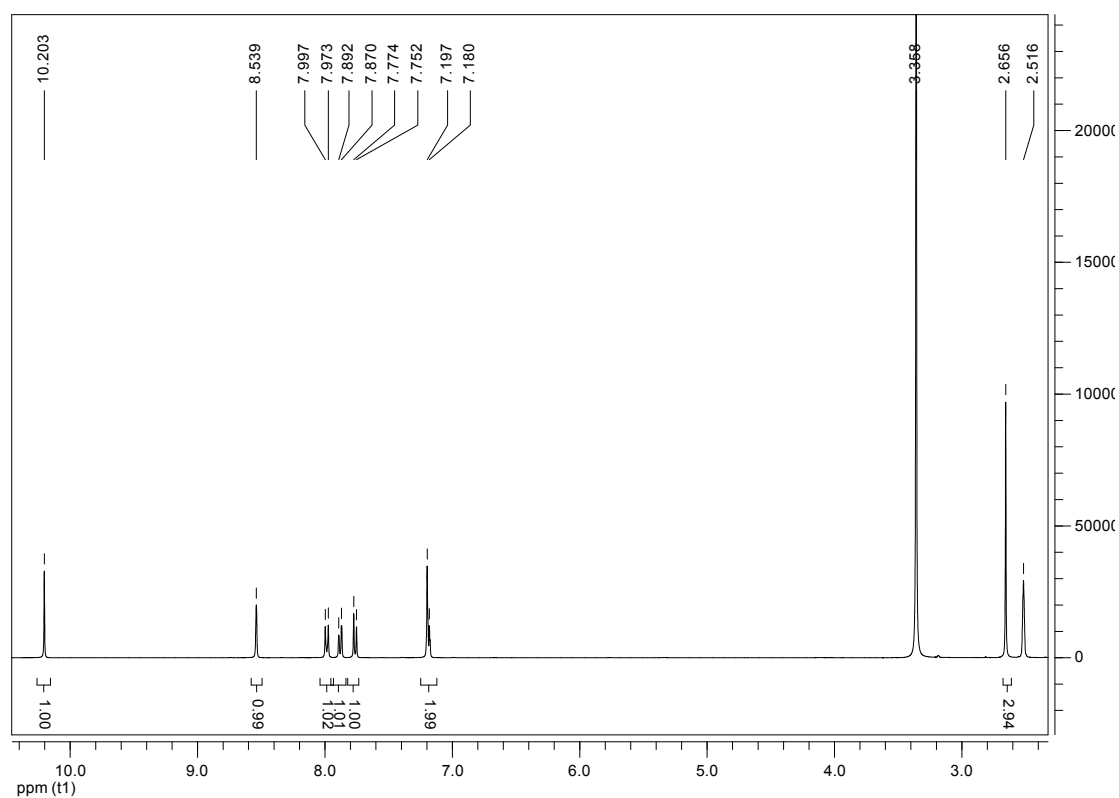


Figure S24. The ¹H NMR spectrum of **11** in DMSO-d₆.

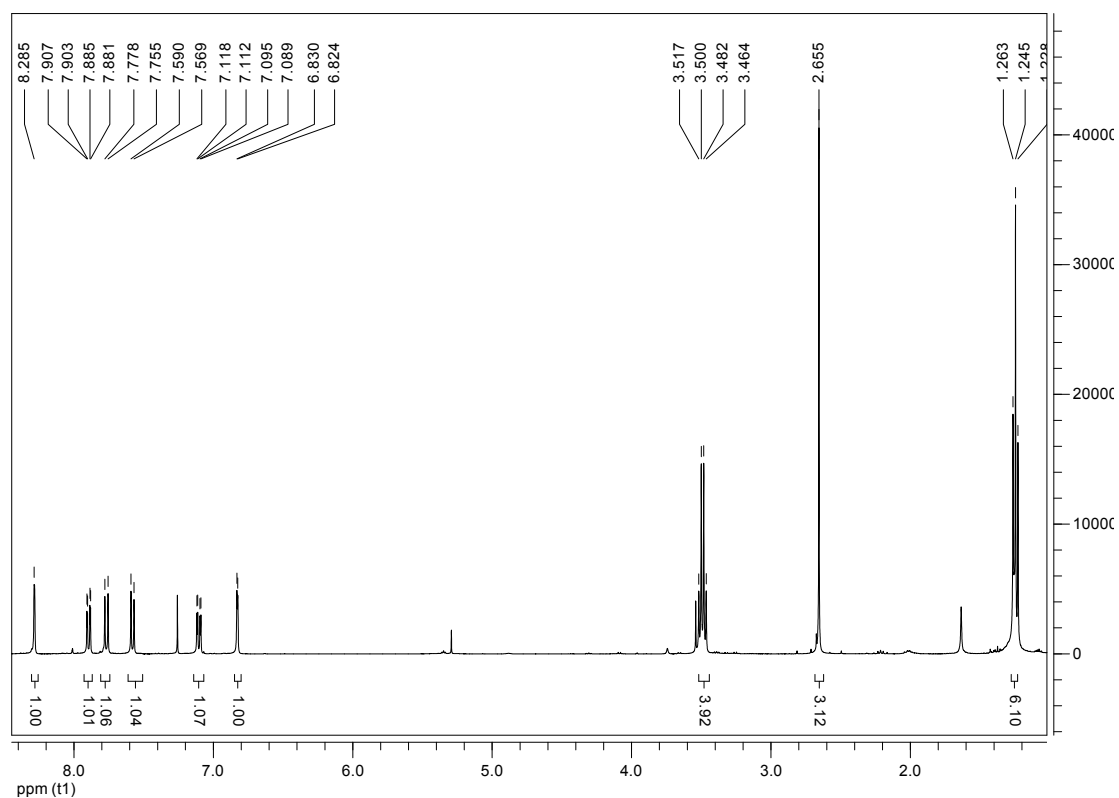


Figure S25. The ¹H NMR spectrum of **12** in CDCl₃.

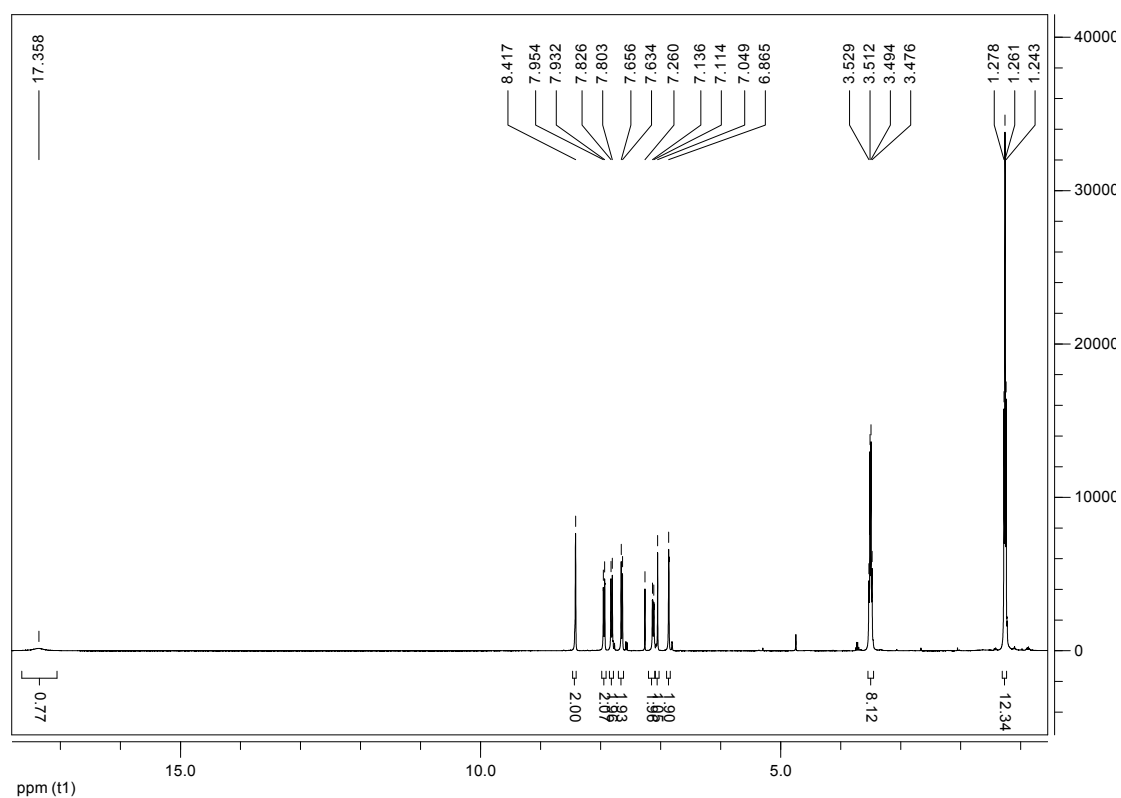


Figure S26. The ^1H NMR spectrum of **13** in CDCl_3 .

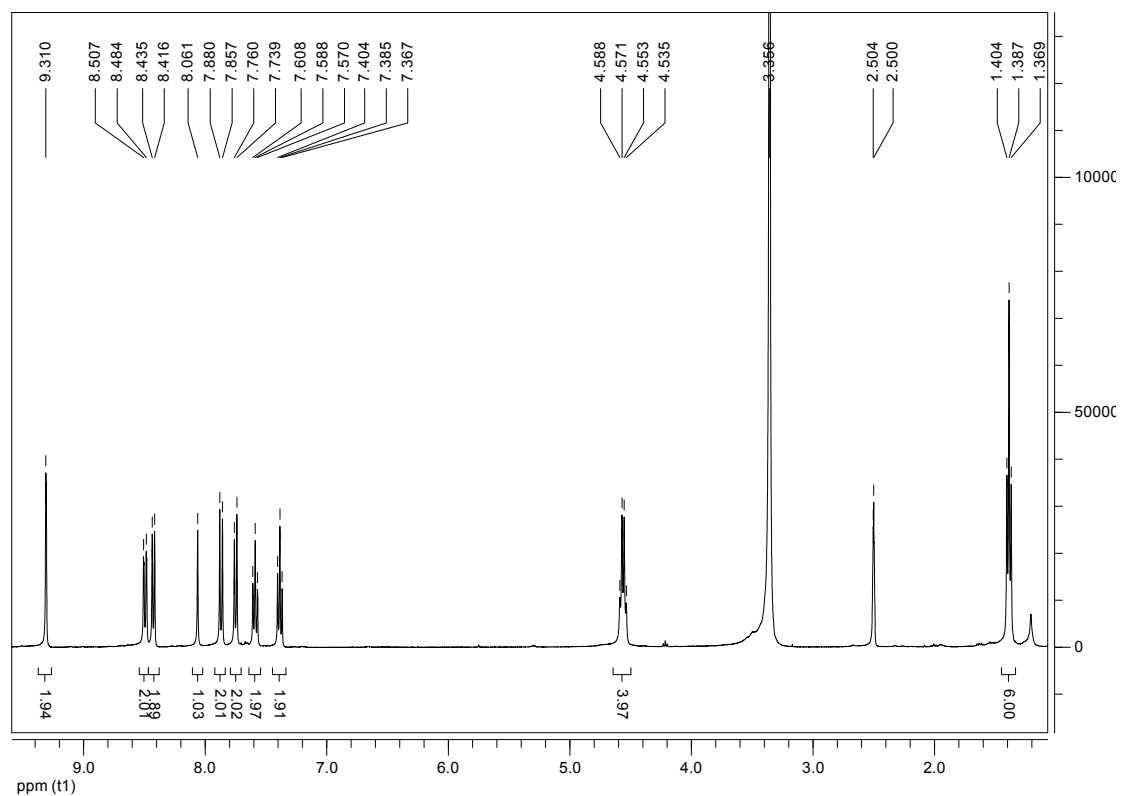


Figure S27. The ^1H NMR spectrum of **BF₂bcz** in DMSO-d_6 .

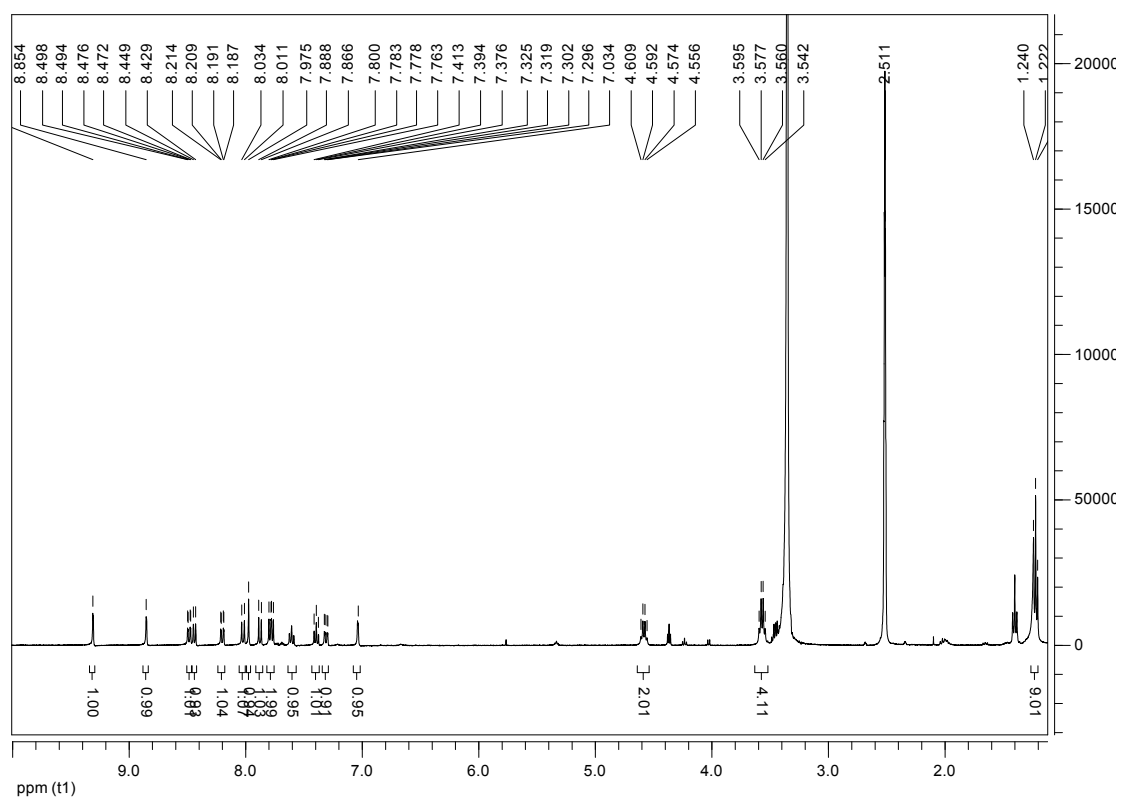


Figure S28. The ^1H NMR spectrum of **BF₂cna** in DMSO-d_6 .

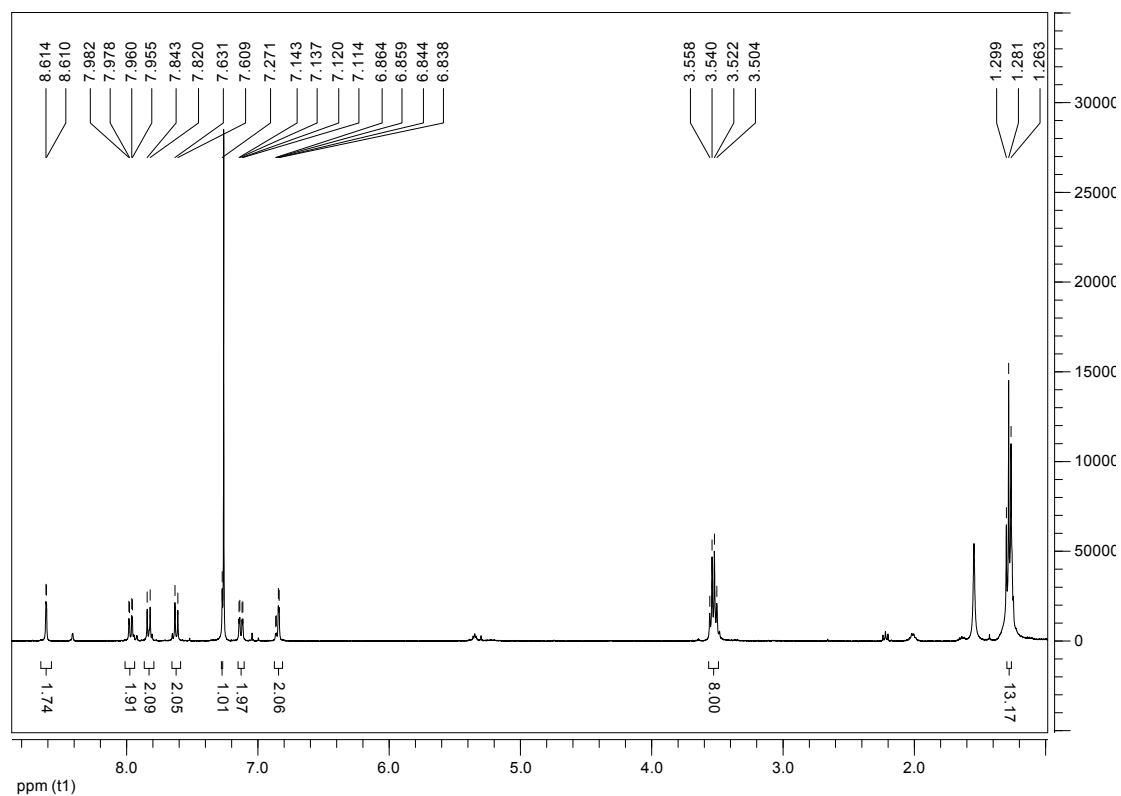


Figure S29. The ^1H NMR spectrum of **BF₂dan** in CDCl_3 .

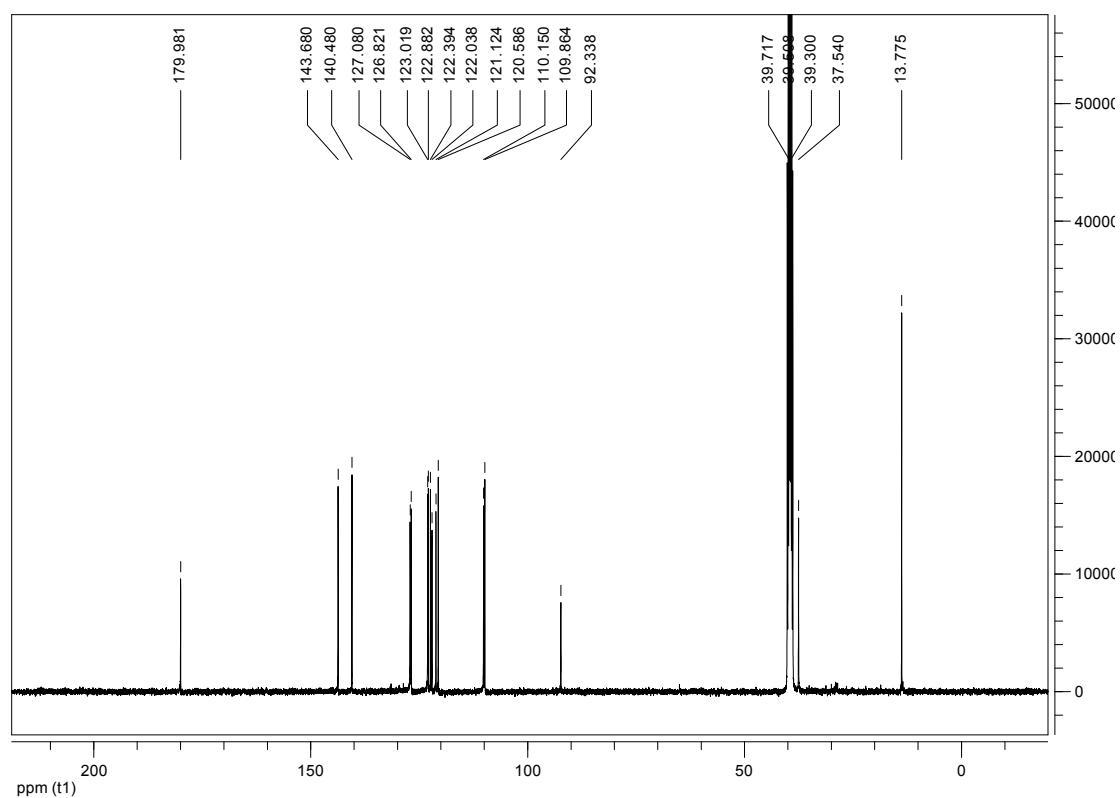


Figure S30. The ^{13}C NMR spectrum of **BF₂bcz** in DMSO- d_6 .

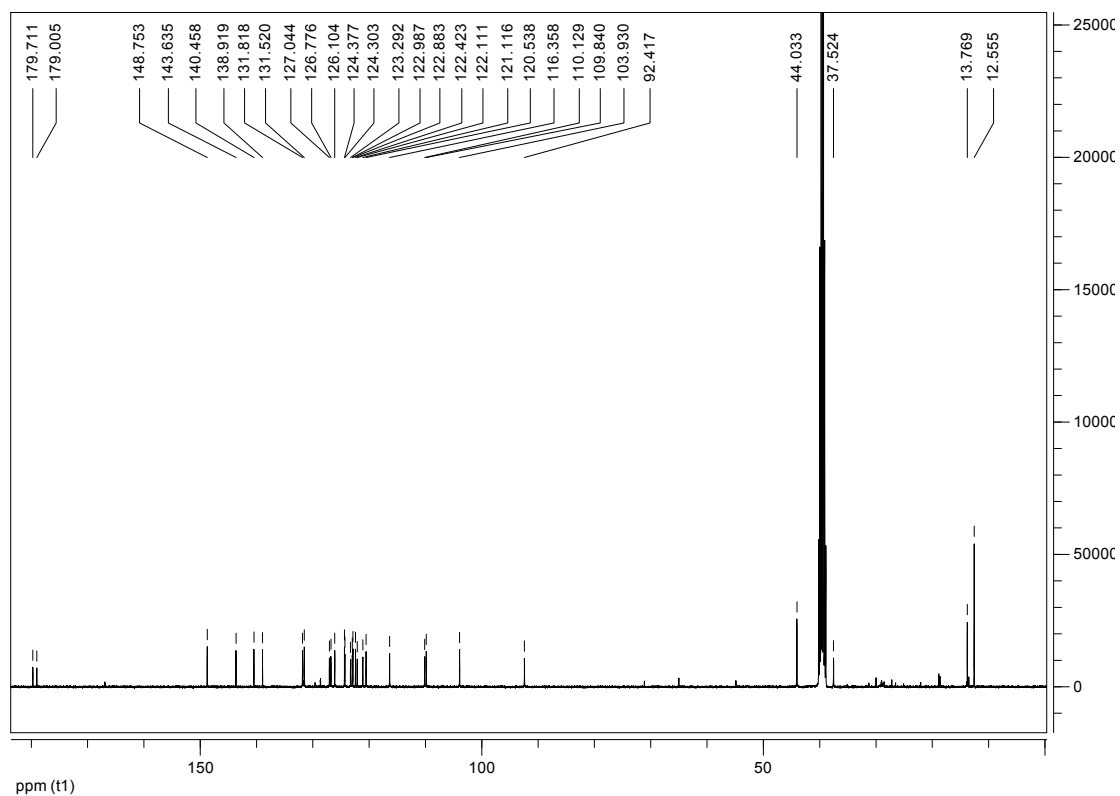


Figure S31. The ^{13}C NMR spectrum of **BF₂cna** in DMSO- d_6 .

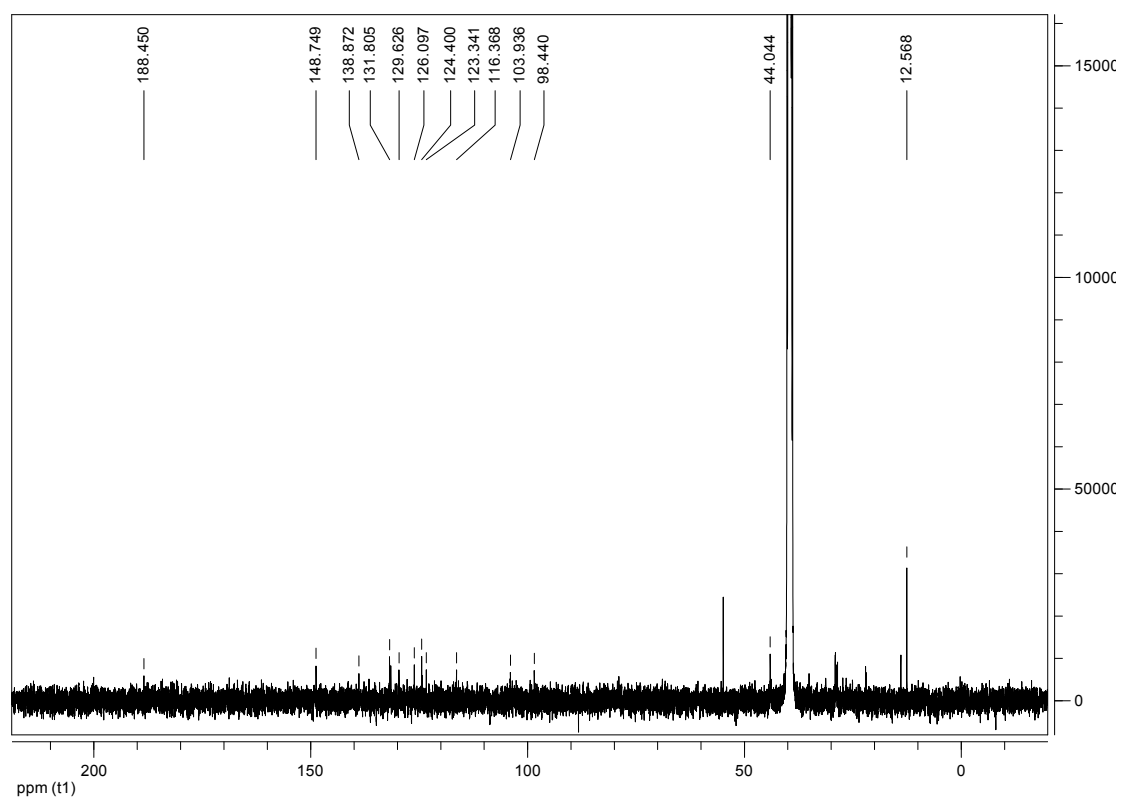


Figure S32. The ¹³C NMR spectrum of BF₂dan in DMSO-d₆.

Analysis Info

Analysis Name 14031249_20140325_000005.d
 Sample 2
 Comment ESI Positive

Acquisition Date 3/25/2014 4:01:11 PM
 Instrument Bruker Apex IV FTMS
 Operator Peking University

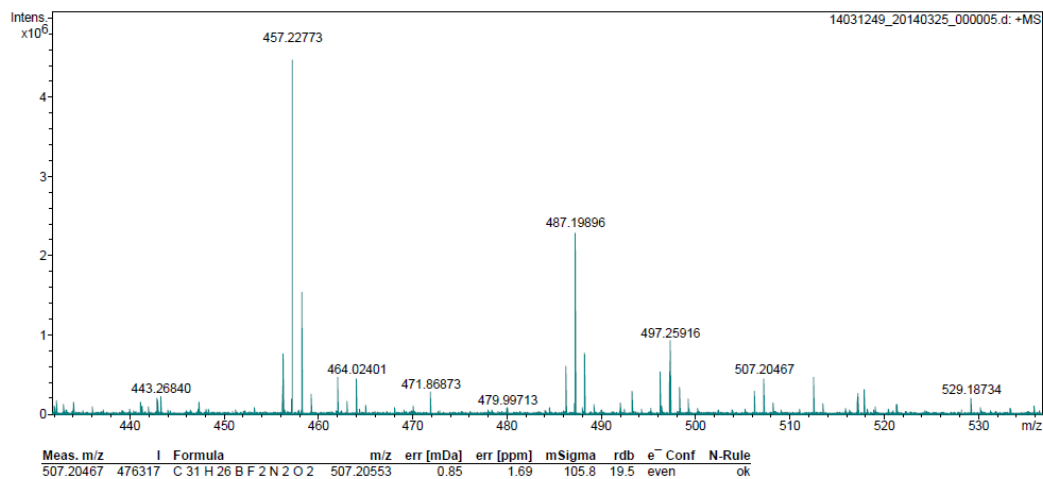


Figure S33. The HR-ESI spectrum of BF₂bcz.

Technical Institute of Physics and Chemistry Mass Spectrometry Sample Analysis Report

Analysis Name: CPZ-19
 Sample: BF₂cna
 Comment: ESI Positive
 Acquisition Date: 1/4/2015
 Instrument: Q-Exactive
 Operator: TIPC
 Chances: 16 #21-25 RT: 0.11-0.13 AM: 5 NL: 2.13E7
 T: FTMS + pESI Full ms [50.00-750.00]

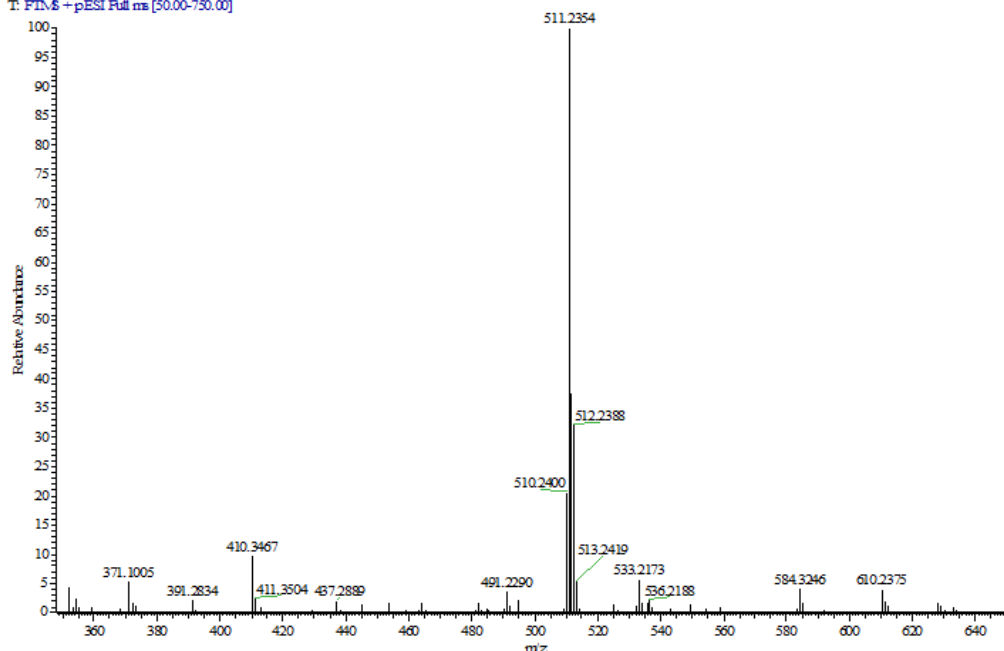


Figure S34. The HR-ESI spectrum of BF₂cna.

Peking University Mass Spectrometry Sample Analysis Report

Analysis Info

Analysis Name: 14120079_20141202_000001.d
 Sample: cpz
 Comment: ESI Positive

Acquisition Date: 12/2/2014 3:41:02 PM
 Instrument: Bruker Apex IV FTMS
 Operator: Peking University

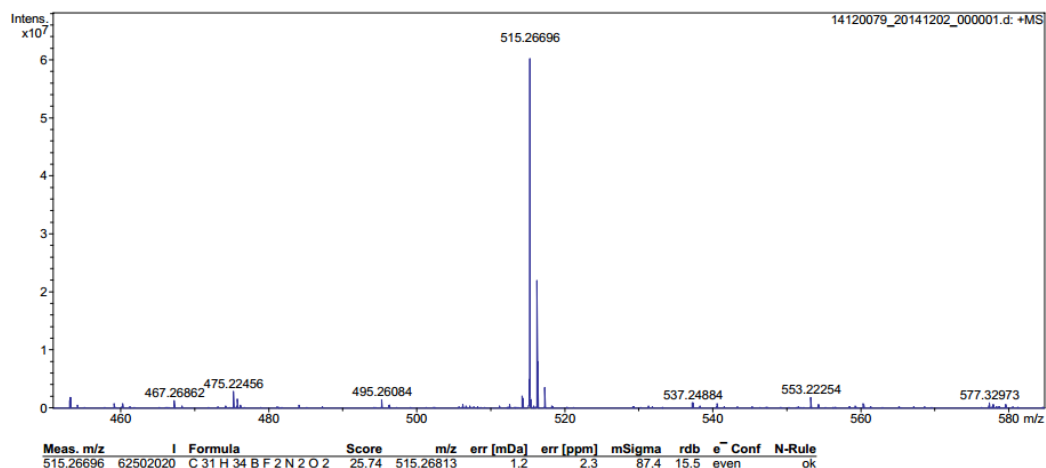
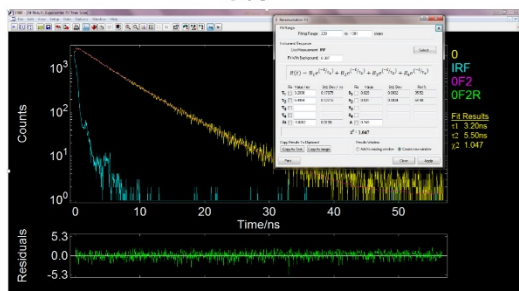


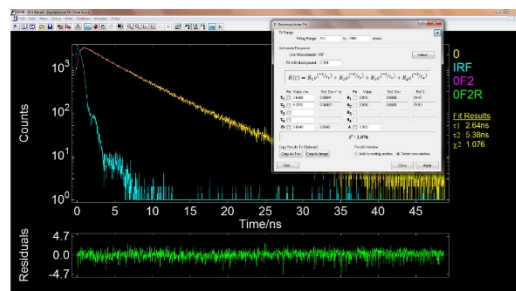
Figure S35. The HR-ESI spectrum of BF₂dan.

5. The lifetime decay profiles of nanocrystals with different ratios of acceptors

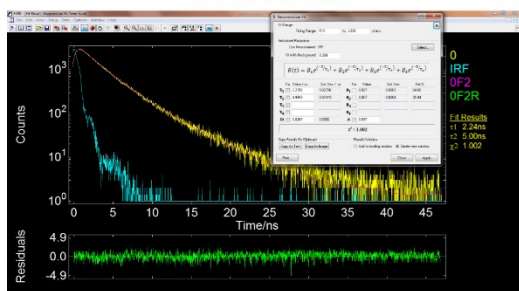
0%



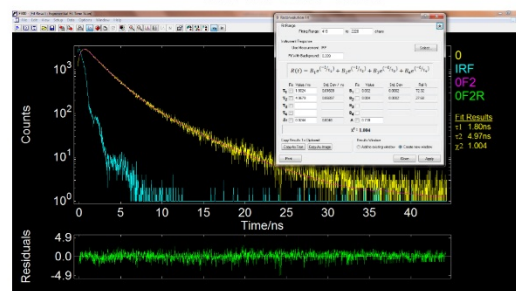
0.001% cna



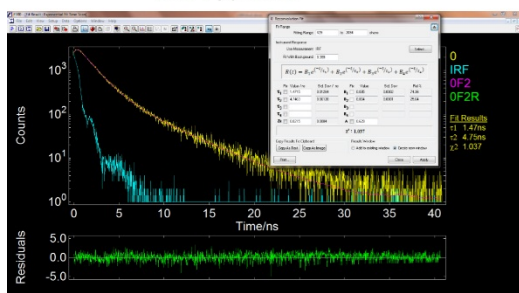
0.005% cna



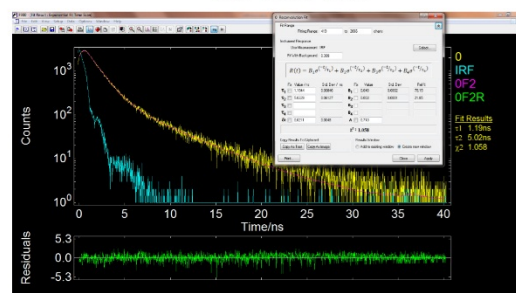
0.0075% cna



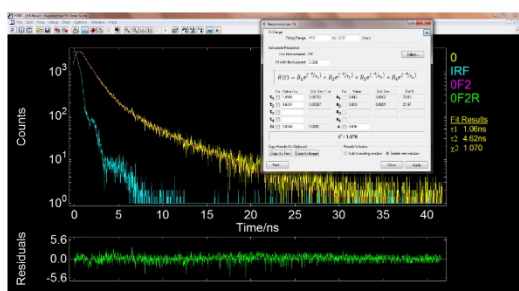
0.01% cna



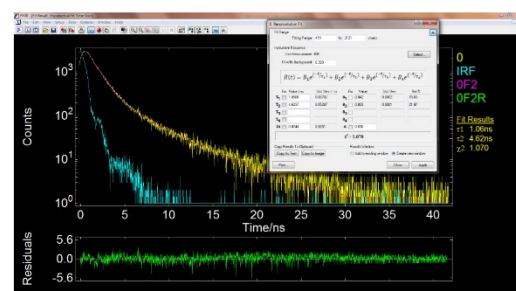
0.015% cna



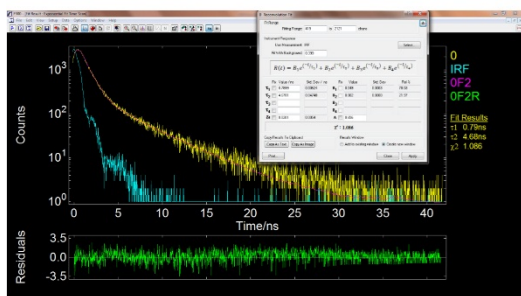
0.02% cna



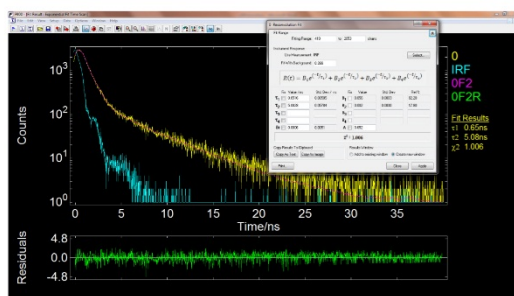
0.025% cna



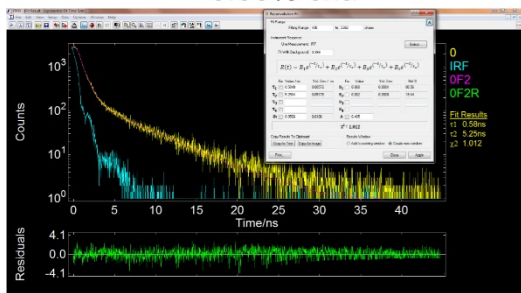
0.03% cna



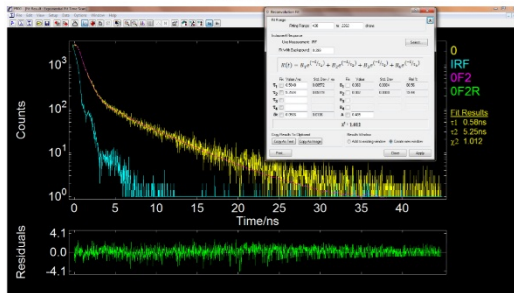
0.04% cna



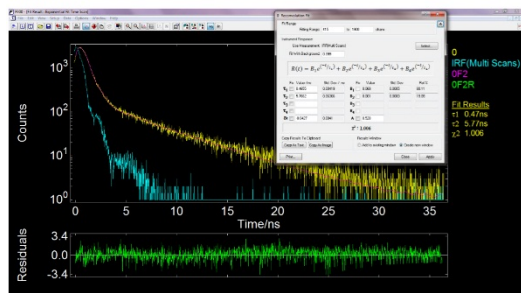
0.05% cna



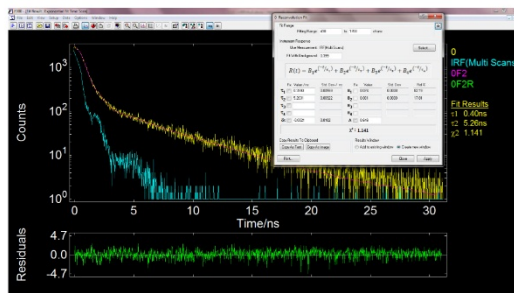
0.06% cna



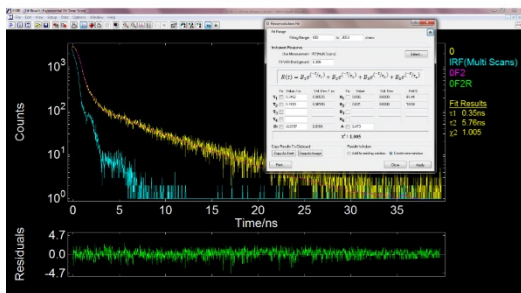
0.07% cna



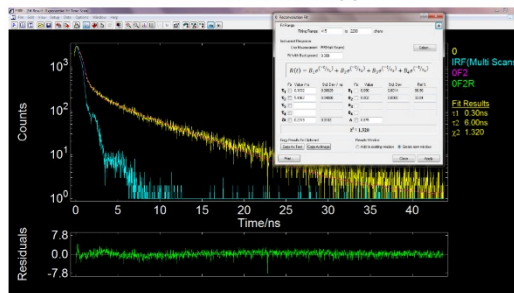
0.08% cna



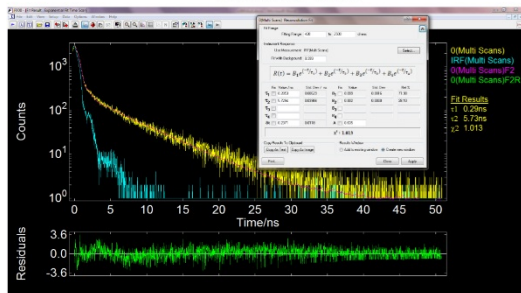
0.09% cna



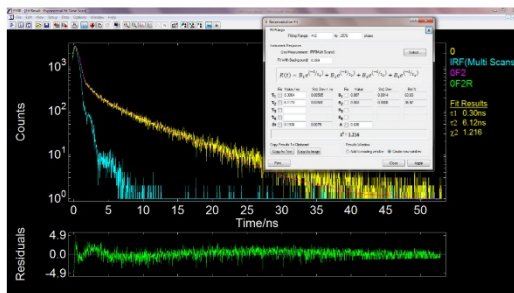
0.11 cna%



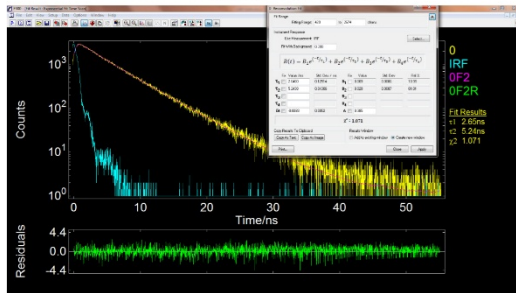
0.13% cna



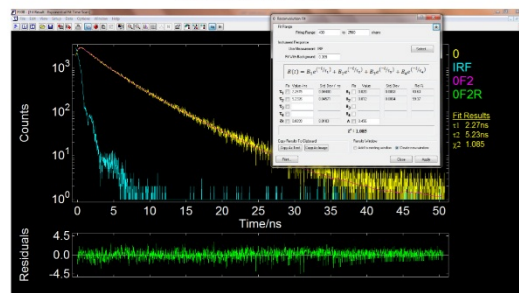
0.15% cna



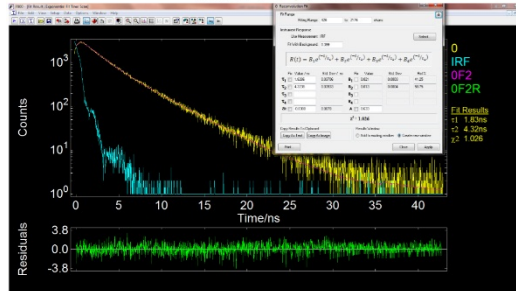
0.001% dan



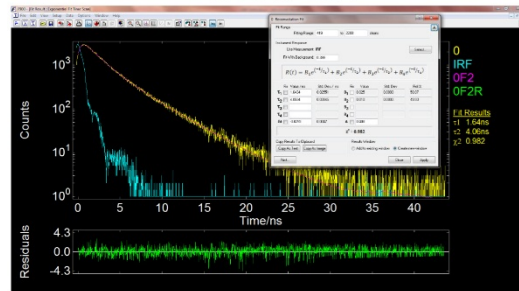
0.005% dan



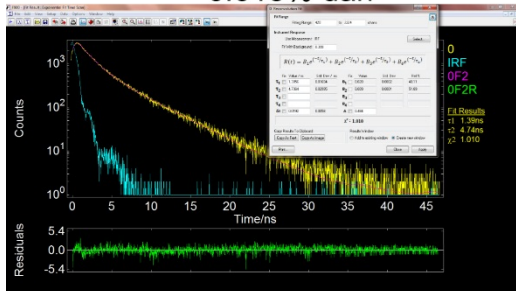
0.0075% dan



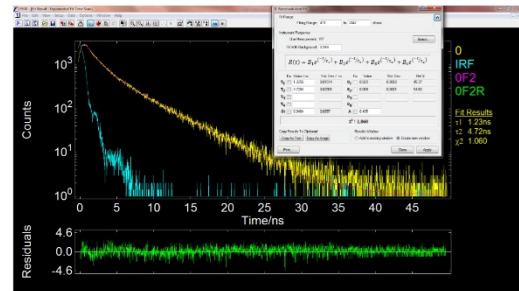
0.01% dan



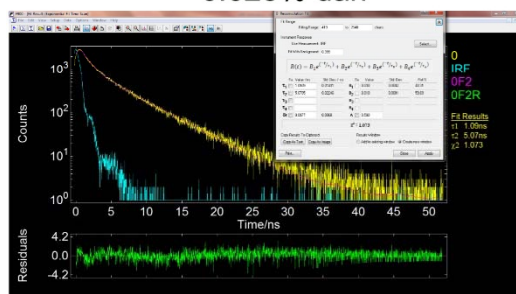
0.015% dan



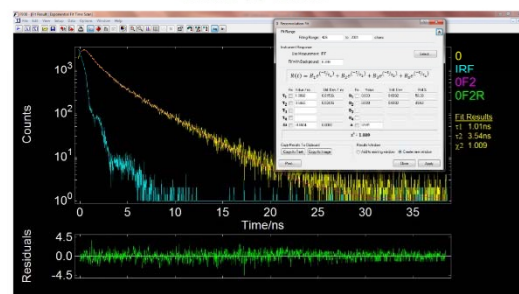
0.02% dan



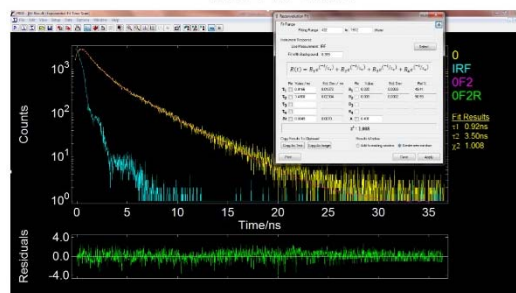
0.025% dan



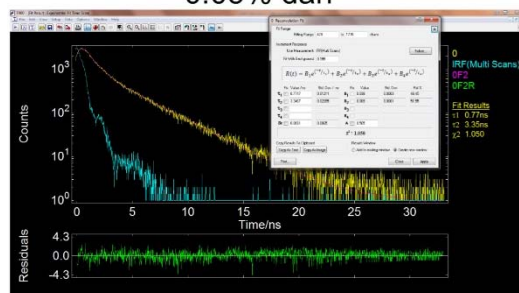
0.03% dan



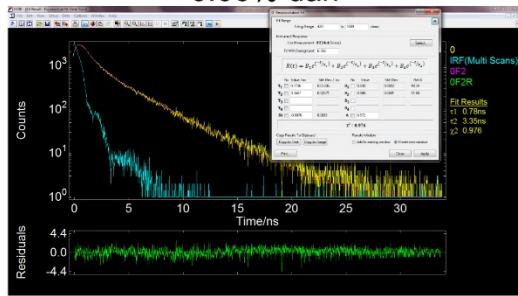
0.04% dan



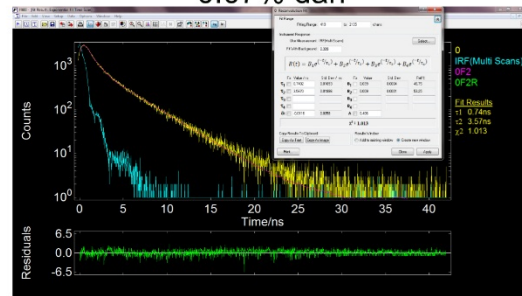
0.05% dan



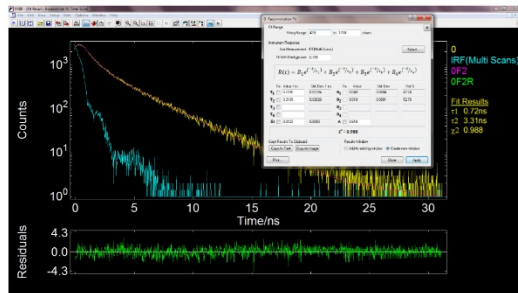
0.06% dan



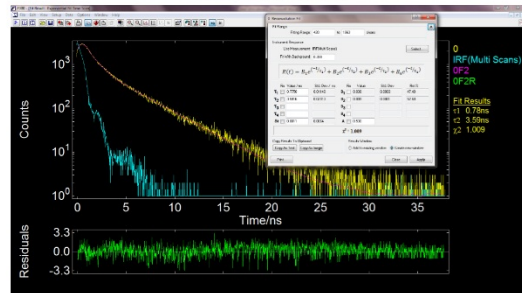
0.07% dan



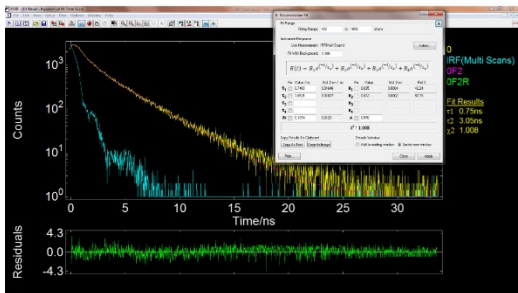
0.08% dan



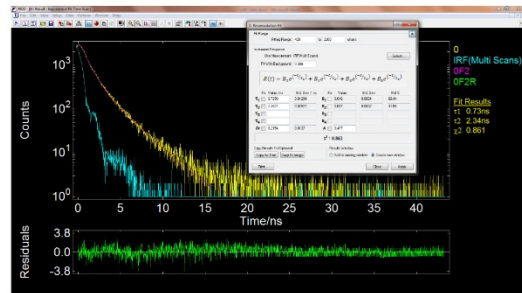
0.09% dan



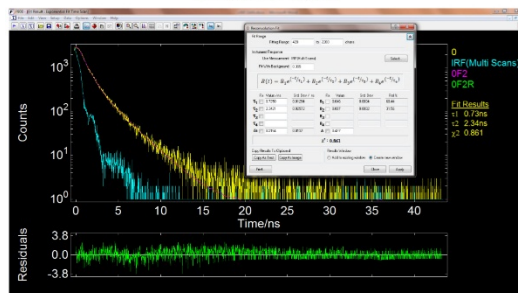
0.11% dan



0.13% dan



0.15% dan



6. References

- [1] M. H. Block, S. Boyer, W. Brailsford, D. R. Brittain, D. Carroll, S. Chapman, D. S. Clarke, C. S. Donald, K. M. Foote, L. Godfrey, A. Ladner, P. R. Marsham, D. J. Masters, C. D. Mee, M. R. O'Donovan, J. E. Pease, A. G. Pickup, J. W. Rayner, A. Roberts, P. Schofield, A. Suleman, A. V. Turnbull, *J. Med. Chem.* **2002**, *45*, 3509-3523.
- [2] G. Bai, J. Li, D. Li, C. Dong, X. Han, P. Lin, *Dyes Pigm.* **2007**, *75*, 93-98.
- [3] A. Petrič, A. F. Jacobson, J. R. Barrio, *Bioorg. Med. Chem. Lett.* **1998**, *8*, 1455-1460.
- [4] a) Y. W. Jun, J. H. Lee, J. S. Choi, J. Cheon, *J. Phys. Chem. B* **2005**, *109*, 14795 - 14806; b) L. T. Kang, H. B. Fu, X. Q. Cao, Q. A. Shi, J. N. Yao, *J. Am. Chem. Soc.* **2011**, *133*, 1895-1901; c) Z. Q. Lin, P. J. Sun, Y. Y. Tay, J. Liang, Y. Liu, N. E. Shi, L. H. Xie, M. D. Yi, Y. Qian, Q. L. Fan, H. Zhang, H. H. Hng, J. Ma, Q. C. Zhang, W. Huang, *Acs Nano* **2012**, *6*, 5309-5319.
- [5] The exciton transport in organic crystal is very complicated (please see references: a) G. Zumofen, A. Blumen, *Chem. Phys. Lett.* **1982**, *88*, 63-67; b) V. M. Kenkre, P. E. Parris, D. Schmid, *Phys. Rev. B* **1985**, *32*, 4946-4955; c) A. Kruger, C. Kryschi, L. Valkunas, D. Schmid, *Chem. Phys.* **1991**, *157*, 243-251). We are currently using ultrafast spectroscopy to further understand the detailed mechanism.
- [6] Y. X. Weng, K. C. Chan, B. C. Tzeng, C. M. Che, *J. Chem. Phys.* **1998**, *109*, 5948-5956.